Bioorganic & Medicinal Chemistry 19 (2011) 7136–7150

Contents lists available at SciVerse ScienceDirect

Bioorganic & Medicinal Chemistry

journal homepage: www.elsevier.com/locate/bmc

2-Anilinonicotinyl linked 2-aminobenzothiazoles and [1,2,4]triazolo[1,5-*b*] [1,2,4]benzothiadiazine conjugates as potential mitochondrial apoptotic inducers

Ahmed Kamal[a,c,*], Y.V.V. Srikanth[a], M. Naseer Ahmed Khan[a], Md. Ashraf[a], M. Kashi Reddy[a], Farheen Sultana[a], Tandeep Kaur[b], Gousia Chashoo[b], Nitasha Suri[b], Irum Sehar[b], Zahoor A. Wani[b], Arpita Saxena[b], Parduman R. Sharma[b], Shashi Bhushan[b], Dilip M. Mondhe[b], Ajit K. Saxena[b]

[a] *Division of Organic Chemistry, Indian Institute of Chemical Technology, Tarnaka, Hyderabad 500607, India*
[b] *Division of Cancer Pharmacology, Indian Institute of Integrative Medicine, Canal Road, Jammu 180001, India*
[c] *Catalytic Chemistry Chair, Chemistry Department, College of Science, King Saud University, Riyadh, Saudi Arabia*

ARTICLE INFO

Article history:
Received 10 August 2011
Revised 28 September 2011
Accepted 29 September 2011
Available online 13 October 2011

Keywords:
2-Anilinonicotinyl-aminothiazoles
Triazolobenzothiadiazines
Cytotoxicity
Cell cycle arrest
Apoptosis
Caspases

ABSTRACT

A series of *N*-(2-anilino-pyridyl) linked 2-amino benzothiazoles (**4a**–**n**) and [1,2,4]triazolo [1,5-*b*]benzothiadiazine conjugates (**5a**–**j**) have been designed, synthesized and evaluated for their antiproliferative activity. Some of these compounds (**4h**–**k**, **4n**, and **5e**) have exhibited potent cytotoxicity specifically against human leukemia HL-60 cell lines with IC_{50} values in the range of 0.08–0.70 μM. All these compounds were tested for their effects on the cell cycle perturbations and induction of apoptosis. Morphological evidences of apoptosis, including fragmentation of nuclei and inter nucleosomal DNA laddering formation were clearly observed after 24 h exposure to compound **4i**. Flow cytometry analysis revealed that compound **4i** showed drastic cell cycle perturbations due to concentration dependant increase in the sub-G0 region which comprises of both the apoptotic and debris fraction, thus implying the extent of cell death. These compounds trigger the mitochondrial apoptotic pathway that results in the loss of mitochondrial membrane potential through activation of multiple caspases followed by activation of caspase-3, and finally cleavage of PARP. Further the mechanism of cell death was analysed by fluorescent microscopic analysis and also by scanning electron microscopy. The cytotoxicity of **4i** correlated with induction of apoptosis, caspases activation and DNA damage and thus indicating the apoptotic pathway of anticancer effect of these compounds.

1. Introduction

Apoptosis or programmed cell death is an orderly cascade that can be regulated and ultimately results in the death of cell in a neat and orderly manner.[1] Recently anticancer efficacy of various chemotherapeutic agents has been correlated with their apoptosis inducing ability. Therefore identification of new molecules that induce apoptosis are attractive for the discovery and development of novel anticancer agents.[2] Nuclear condensation and DNA fragmentation by different biological as well as cytological processes are involved in the apoptosis.[3] Caspases are a family of cysteine proteases and are known to play a critical role for the initiation and execution of apoptosis.[4] Amongst the caspases, caspase-3, -6, and -7 are the key effector caspases that cleave multiple protein substrates in the cells that lead to irreversible cell death.[5]

E7010 (**1**) is a sulfonamide, which inhibits tubulin polymerization[6] (Fig. 1) and causes cell cycle arrest and apoptosis in M phase.[7,8] This compound exhibits good in vivo antitumour activity against several rodent as well as human tumours and is in phase II clinical studies.[9] *N*-Phenyl nicotinamides (**2**) are a new class of apoptosis inducers that are known to arrest cells in G2/M phase and structure–activity relationship (SAR) studies indicate that the 3-pyridyl group is very important for their activity.[10] Recently we synthesised a new family of 2-anilinonicotinyl arylsulfonyl hydrazides that exhibit promising antitumour activity.[11] Whereas benzothiazoles are known to exhibit various biological properties including antimicrobial, anticancer, antiamyloid, antirheumatic and antiglutamate activities.[12–15] Various arylbenzothiazoles and aminobenzothiazoles are also known to possess promising anticancer activity both in vivo and in vitro models.[16–20] More recently, Re and Tc metal complexes conjugated to the antitumour agent 2-(4-aminophenyl) benzothiazole have been evaluated as potential candidates for imaging (^{99}mTc) and targeted radiotherapy (^{188}Re) of breast cancer.[21] A series of cyano substituted

---

* Corresponding author. Tel.: +91 40 27193157; fax: +91 40 27193189.
E-mail address: ahmedkamal@iict.res.in (A. Kamal).

0968-0896/$ - see front matter © 2011 Elsevier Ltd. All rights reserved.
doi:10.1016/j.bmc.2011.09.060

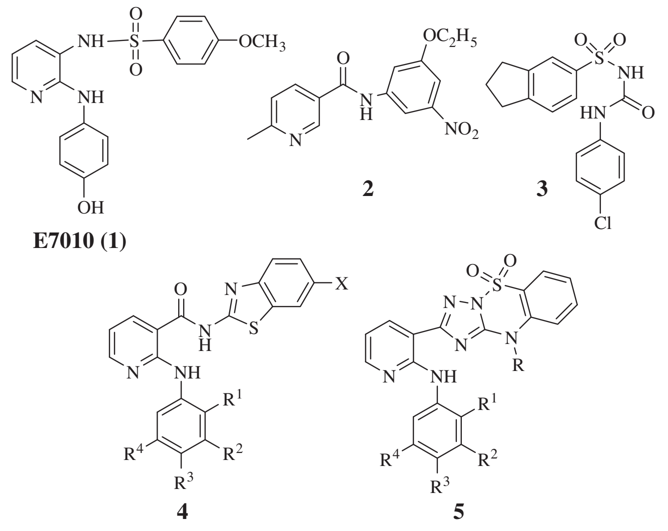

Figure 1. Chemical structures of E7010 (**1**), *N*-phenyl nicotinamides (**2**), sulofenur (**3**), **4** and **5**.

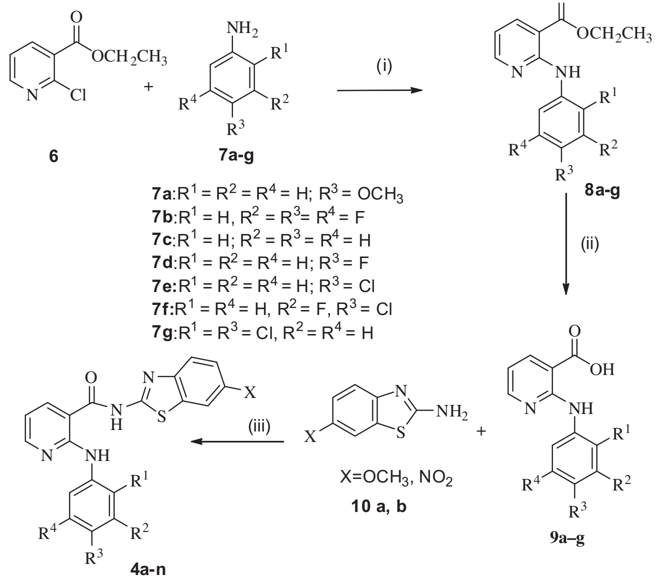

7a: $R^1 = R^2 = R^4 = H$; $R^3 = OCH_3$
7b: $R^1 = H$, $R^2 = R^3 = R^4 = F$
7c: $R^1 = H$; $R^2 = R^3 = R^4 = H$
7d: $R^1 = R^2 = R^4 = H$; $R^3 = F$
7e: $R^1 = R^2 = R^4 = H$; $R^3 = Cl$
7f: $R^1 = R^4 = H$, $R^2 = F$, $R^3 = Cl$
7g: $R^1 = R^3 = Cl$, $R^2 = R^4 = H$

4a: $R^1 = R^2 = R^4 = H$; $R^3 = OCH_3$
4b: $R^1 = H$, $R^2 = R^3 = R^4 = F$
4c: $R^1 = H$; $R^2 = R^3 = R^4 = H$
4d: $R^1 = R^2 = R^4 = H$; $R^3 = F$
4e: $R^1 = R^2 = R^4 = H$; $R^3 = Cl$
4f: $R^1 = R^4 = H$, $R^2 = F$, $R^3 = Cl$
4g: $R^1 = R^3 = Cl$, $R^2 = R^4 = H$
$X = OCH_3$

4h: $R^1 = R^2 = R^4 = H$; $R^3 = OCH_3$
4i: $R^1 = H$, $R^2 = R^3 = R^4 = F$
4j: $R^1 = H$; $R^2 = R^3 = R^4 = H$
4k: $R^1 = R^2 = R^4 = H$; $R^3 = F$
4l: $R^1 = R^2 = R^4 = H$; $R^3 = Cl$
4m: $R^1 = R^4 = H$, $R^2 = F$, $R^3 = Cl$
4n: $R^1 = R^3 = Cl$, $R^2 = R^4 = H$
$X = NO_2$

Scheme 1. Reagents and conditions: (i) ethylene glycol, 160 °C, 6 h; (ii) 2 N NaOH, ethanol, reflux 2 h; (iii) EDCI/HOBt, dry DMF 0 °C to rt, 8 h.

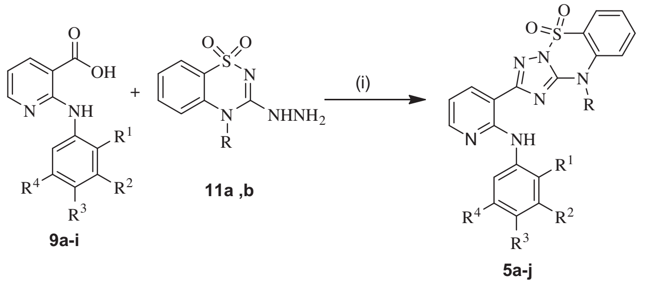

5a: $R = CH_3$, $R^1 = R^2 = R^4 = H$, $R^3 = OCH_3$
5b: $R = CH_3$, $R^1 = H$, $R^2 = R^3 = R^4 = F$
5c: $R = CH_3$, $R^1 = R^2 = R^3 = R^4 = H$
5d: $R = CH_3$, $R^1 = R^2 = R^4 = H$, $R^3 = Cl$
5e: $R = CH_3$, $R^2 = R^4 = H$, $R^1 = R^3 = Cl$
5f: $R = Ph$, $R^1 = R^2 = R^4 = H$, $R^3 = OCH_3$
5g: $R = Ph$, $R^1 = H$, $R^2 = R^3 = R^4 = F$
5h: $R = Ph$, $R^1 = R^2 = R^3 = R^4 = H$
5i: $R = Ph$, $R^2 = R^4 = H$, $R^1 = R^3 = Cl$
5j: $R = Ph$, $R^1 = R^2 = R^4 = H$, $R^3 = Cl$

Scheme 2. Reagents and conditions: (i) $POCl_3$, 105 °C, 3 h.

amidinobenzothiazole derivatives are also reported to exhibit potential anticancer activity.[22] Sulfonylurea derivatives represent another important class of biologically active compounds with a broad spectrum of activity in several solid tumour models.[23] A compound from this class, sulofenur (LY186641, **3**) has been clinically evaluated in many cancer cell lines.[24–26] These compounds are known to exert their biological effect by inhibiting DNA, RNA, or protein synthesis.[27,28] Many cyclic sulfonamide derivatives of [1,2,4]triazolo [1,2,4]benzothiadiazine scaffold possess interesting anticancer properties.[29,30]

Our earlier efforts towards the synthesis of a variety of hybrid molecules led to the development of efficient anticancer agents.[31–35] Based on these findings an attempt has been made in the present study to incorporate a 2-aminobenzothiazole moiety, as well as the triazolo fused [1,2,4]benzothiadiazines to the 2-anilino pyridyl structural component of E7010 (**1**). We hypothesized that 2-anilinonicotinyl moiety and aminobenzothiazoles or triazolobenzothiadiazine scaffolds within a single molecule could enhance the cytotoxic effect, therefore we synthesized *N*-(2-anilino-pyridyl) linked 2-aminobenzothiazoles (**4**) and [1,2,4]triazolo [1,5-*b*]benzothiadiazines (**5**) and evaluated for their antiproliferative activity (Fig. 1). Moreover, they have been investigated for their effect on cell cycle perturbations and induction of apoptosis.

2. Results and discussions

2.1. Chemistry

Compounds (**4a**–**n**) were prepared as shown in Scheme 1. 2-Chloronicotinic acid ethyl ester (**6**) and substituted anilines (**7a**–**g**) were refluxed in ethylene glycol to provide 2-anilino nicotinic acid esters (**8a**–**g**), which on treatment with 2 N NaOH solution in ethanol afford the corresponding 2-anilino nicotinic acids (**9a**–**g**) in quantitative yields. The synthesis of the desired products (**4a**–**n**) was carried out by the reaction of the respective 2-anilino nicotinic acids with 6-substituted 2-amino benzothiazoles (**10a**,**b**) with EDCI/HOBt in dry DMF as solvent.

Compounds (**5a**–**j**) were prepared as illustrated in Scheme 2. The preparation of the starting materials, that is 3-hydrazino-4-methyl/phenyl-4*H*-1,2,4-benzothiadiazine 1,1-dioxides (**11a**,**b**) was accomplished by the previously synthetic sequence.[36] The synthesis of triazolo fused benzothiadiazines (**5a**–**j**) was carried out by refluxing **11a**,**b** with 2-anilino nicotinic acids (**9a**–**i**) in phosphorous oxychloride.

2.2. Biological results

2.2.1. In vitro anti proliferative activity

Preliminary screening of all the synthesized compounds was evaluated for their activity against a panel of 10 different human cancer cell lines (IMR-32, SK-NS-H, SiHa, SW-620, HCT-15, 502713, DU-145, A-549, HEp-2 and OVCAR-5) using sulforhodamine B (SRB) method.[37] The test compounds were added at a single dose of 10 μM concentration and results were calculated as percent inhibition of cell proliferation. Paclitaxel, 5-fluorouracil and mitomycin C were used as positive controls in this assay. Some of the compounds have exhibited potential growth inhibitory effect in almost all the cell lines. Benzothiazole analogues (**4a**–**n**) have shown better growth inhibitory potency than their corresponding triazolobenzothiadiazine analogues (**5a**–**j**) as seen from Table 1. Compound **4i** was found to be the most potent amongst the series that exhibited more than 50% growth inhibition against most of the cancer cell lines. Interestingly, compounds with nitro substituent in the benzothiazole ring showed better potency in comparison to the compounds with methoxy substituent. Moreover, introduction of a fluorine atom in the anilino ring of the nicotinyl moiety enhanced the inhibitory effect.

2.2.2. Cytotoxicity of the representative potential compounds

Compounds such as **4h**–**k**, **4n,** and **5e** that exhibit efficient antiproliferative activity in the preliminary screening were evaluated for their cytotoxicity against three representative human cancer cell lines of leukemia (HL-60) and cervix (SiHa) at concentrations up to 50 μM using MTT assay.[38] Interestingly, all the six compounds displayed substantial cytotoxicity towards the leukemia cell line HL-60 with IC_{50} values in the range of 0.08–0.7 μM (Table 2) and compound **4i** exhibited highest cytotoxicity with IC_{50} value of 0.08 μM. These compounds exhibited moderate to good cytotoxicity against cervical cancer cell line with IC_{50} value up to 7 μM. Further, to investigate therapeutic ratio of the compounds, we examined the cytotoxicity in normal cell line of monkey kidney (CV-1). The cytotoxic potential of these compounds was weak or limited except compound **4l** with IC_{50} value of 0.8 μM. The high therapeutic ratio of compound **4i** shows its in vitro antigrowth activity is 1250 times higher in leukemia cell line HL-60 than in normal cells (CV-1). Thus it has a high safety window and provides a significant therapeutic benefit particularly as an antileukemic agent. In view of the promising antitumour activity and higher therapeutic ratio amongst the compounds evaluated it was

Table 2
Cytotoxicity in cancer cells and normal cells and their comparison

In-vitro growth inhibitory IC_{50} values[a] (μM)				
	Cancer cell lines		Normal cell lines	Therapeutic ratio
Compd	HL-60[b]	SiHa[c]	CV-1[d]	(CV-1/HL-60)
4h	0.70	28	10	14
4i	0.08	36	>100	>1250
4j	0.58	28	70	120
4k	0.30	7	15	50
4l	0.40	>50	0.8	2
5e	0.64	>50	>100	>156

[a] Mean of three determinations.
[b] Leukemia cell line.
[c] Cervical cancer cell line.
[d] Monkey kidney normal cell line.

Table 1
Percentage of growth inhibition[a] for selected cancer cell lines by **4a**–**n** and **5a**–**j** compounds at 10 μM concentrations

Compd	IMR-32[b]	SK-NS-H[b]	SiHa[c]	SW-620[d]	HCT-15[d]	502713[d]	DU145[e]	A549[f]	HEp-2[g]	OVCAR-5[h]
4a	40	44	55	43	0	21	22	20	0	8
4b	55	47	63	52	21	43	28	6	7	25
4c	26	26	63	29	0	11	25	9	33	6
4d	2	24	35	21	0	2	32	5	32	3
4e	24	23	31	15	44	10	25	10	13	10
4f	21	42	40	30	20	7	33	26	11	9
4g	6	14	16	10	24	4	17	0	17	4
4h	55	64	66	64	47	59	32	3	5	52
4i	72	49	70	70	62	80	39	27	0	52
4j	45	48	53	65	66	63	52	31	26	50
4k	33	63	23	67	55	66	51	18	52	53
4l	45	48	53	65	66	63	52	83	69	26
4m	3	3	13	34	0	28	9	78	61	3
4n	48	50	35	61	75	2	39	19	14	0
5a	15	20	11	24	0	13	8	70	13	4
5b	28	18	15	34	9	26	13	14	0	8
5c	0	0	0	32	0	30	8	39	0	15
5d	3	3	13	34	0	28	9	28	0	10
5e	47	16	13	62	27	49	11	15	0	23
5f	0	0	0	14	0	2	5	0	10	2
5g	48	16	26	22	0	14	14	3	52	2
5h	56	20	23	23	0	21	10	0	0	3
5i	11	23	23	27	0	19	20	66	25	8
5j	31	27	30	68	0	18	6	46	57	1
Pac[i]	46	20	49	73	37	59	42	41	–[l]	51
5-FU[j]	71	7	44	76	44	21	–[l]	–[l]	–[l]	22
Mito-c[k]	–[l]	–[l]	–[l]	–[l]	–[l]	–[l]	44	34	7	–[l]

[a] Mean values from three independent experiments.
[b] Neuroblastoma cancer cell line.
[c] Cervical cancer cell line.
[d] Colonic adenocarcinoma cell line.
[e] Prostate cancer cell line.
[f] Lung cancer cell line.
[g] Larynx carcinoma.
[h] Ovary cancer cell line.
[i] Paclitaxel.
[j] 5-Fluorouracil.
[k] Mitomycin C.
[l] Not evaluated in the corresponding cell line.

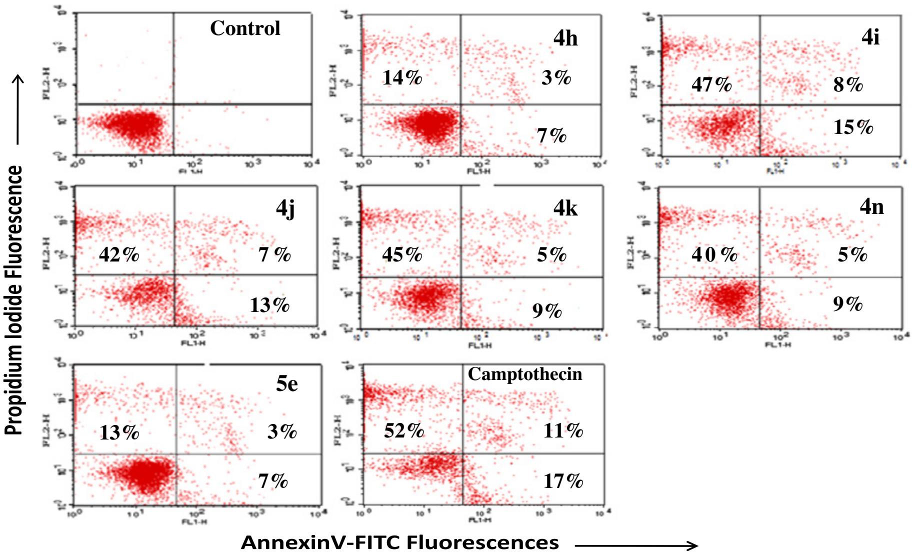

Figure 2. Annexin V-PI analysis in HL-60 cells, following 24 h of drug treatment of compounds **4h**–**k**, **4n**, and **5e** at 1 μM by Annexin-V-FITC method. The number of Annexin -V-positive cells was determined using a flow cytometer and the percentage is represented in each panel. Each condition was analyzed in a histogram which displays two parameters, Annexin V-FITC and PI, as represented. The dual parametric dot plots show the viable cell population in the lower left quadrant (Annexin V-negative/PI-negative), the early apoptotic cells in the lower right quadrant (Annexin V-positive/PI-negative), and the late apoptotic cells in the upper right quadrant (Annexin V-positive/PI-positive). Results are representative of one of three independent experiments.

considered of interest to pursue further studies on these compounds to find a potential lead.

2.3. Induction of apoptosis

2.3.1. Annexin V-FITC/Propidium iodide analysis of apoptosis

During apoptosis an important biochemical change that takes place in cells is flipping of the phosphatidyl serine (PS) lipid from the inner leaflet of the cellular membrane to the outer one. Annexin V, a calcium-dependent phospholipids binding protein has a high affinity for PS. Hence FITC-labeled Annexin V has been used in the flow cytometric detection to identify apoptotic cells. Compounds **4h**–**k**, **4n,** and **5e** were treated with HL-60 cells at 1 μM concentration and incubated for 24 h. The extent of apoptosis vs necrosis was analyzed from the quadrant analysis of cell population with Annexin V-FITC. Both the apoptotic and post apoptotic cell populations increased in HL-60 cells. All the compounds induce apoptosis whereas compound **4i** provoked a significant apoptotic induction in HL-60 cells after 24 h treatment. These results prompted us to further investigate the mechanism involved in the process of apoptosis (Fig. 2).

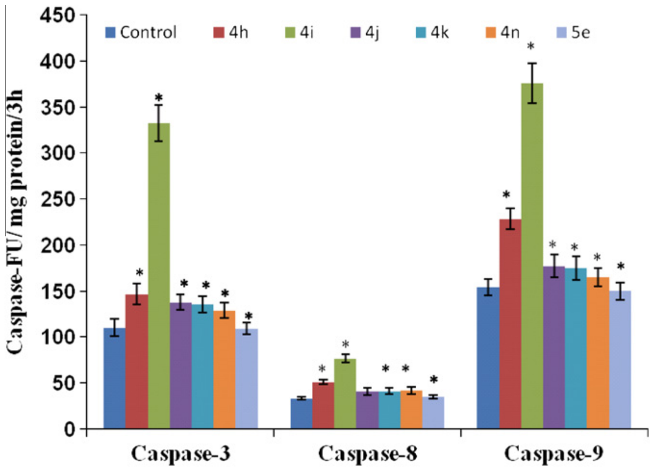

Figure 3. Effect of compounds on caspase-3, -8 and -9 activities in HL-60 cells determined by fluorimetry at 1 μM after 24 h incubation. Error bars represents data from two independent experiments with each performed in duplicate. Data are mean ± SD from three independent experiments. *p*-value: *<0.05 compared to untreated control through ANOVA test.

2.3.2. Activation of caspase induction

Most of the proteolytic cleavages during apoptosis result from the activation of caspases, a family of cysteine-dependent proteases. Caspases can initiate apoptotic signals and execute the apoptotic programs.[39] Hence, the involvement of various caspases and their role in the process of apoptosis has been investigated. Compounds that showed apoptosis induction in the Annexin V flow cytometric assay were also evaluated for their ability to induce caspase activity in HL-60 cells. Compound **4i** upon treatment at 1 μM concentration for 24 h in HL-60 cells activated caspases-3, -8, and -9 by 2–3 folds (Fig. 3), whereas other compounds (**4h**, **4j**, **4k**, **4n**, and **5e**) showed negligible induction of apoptosis in the Annexin V assay and marginal activation of caspases. The activation of both caspase-9 and caspase-8 by **4i** indicates that it induces apoptosis through both the intrinsic as well as extrinsic apoptotic pathway in HL-60 cells.

2.3.3. DNA fragmentation

Apoptosis was also assessed by electrophoresis of extracted genomic DNA from cells. Endonuclease mediated cleavage of nuclear DNA results in the formation of oligonucleosomal DNA fragment (180–200 base pairs long) a biochemical hallmark of apoptosis[40] in many cell types. DNA laddering assay was performed with HL-60, SiHa and HeLa cells by treatment of compounds **4h**–**k**, **4n**, and **5e** at concentrations 1 and 10 μM for 24 h, then the genomic DNA was isolated and electrophoresed in a 1.8% agarose gel (Figs. 4 and 5). All the tested compounds induce DNA fragmentation that is, characteristic ladder pattern in HL-60 cells at 1 and 10 μM. While no laddering was observed in cervical cancer cells (SiHa and HeLa) even at higher concentrations (10 μM), thus indicating that these compounds specifically target the leukemia cells (HL-60).

2.3.4. Cell cycle effects

DNA fragmentation is one of the hallmarks of biochemical changes seen in apoptotic cell death. Thus, measurement of DNA

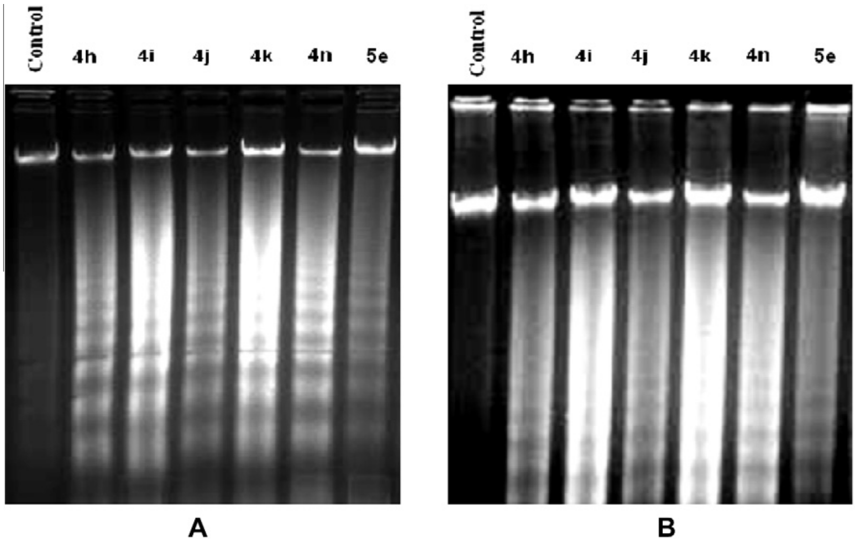

Figure 4. Effect of compounds **4h**–**k**, **4n**, and **5e** on DNA fragmentation on leukemia cells (HL-60). Cells were incubated for 24 h with 1 and 10 μM concentrations (A and B, respectively). The treated and control cells were incubated for 24 h in the regular culture media, after which time the DNA was prepared and then applied to 1.8% agarose gel electrophoresis. Internucleosomal DNA fragmentation was visualized under UV light in Bio-Rad gel documentation system.

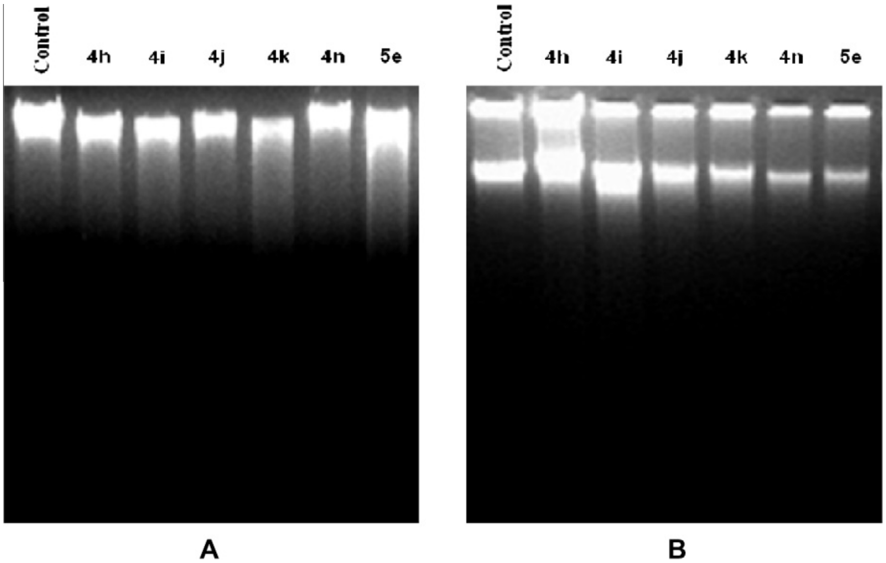

Figure 5. Effect of compounds **4h**–**k**, **4n**, and **5e** on DNA fragmentation on SiHa (**A**) and HeLa (**B**) cells. Cells were incubated for 24 h with 10 μM concentration. The treated and control cells were incubated for 24 h in the regular culture media, after which time the DNA was prepared and then applied to 1.8% agarose gel electrophoresis. Internucleosomal DNA fragmentation was visualized under UV light in Bio-Rad gel documentation system.

content makes it possible to identify apoptotic cells, to recognize the cell cycle phase specificity and to quantitate apoptosis. HL-60 cells upon exposure to 1 μM concentration of these compounds for 24 h exhibited continuous increase in sub-G0 fraction that may comprise of both apoptotic and debris fraction implying together the extent of cell death (Fig. 6a). The damage was more apparent with compound **4i** and **4k** (94% and 60% DNA damaged, respectively, Figure 6b). These compounds did not produce mitotic block or delay in cell cycle and there was a significant fall in relative PI fluorescence of cell fractions in all the three phases G1, S and G2/M, thus indicating that the decrease in DNA fluorescence is not cell cycle selective.

2.3.5. Mitochondrial generation of intracellular peroxides in HL-60 cells

Apoptosis can be initiated by oxidative stress which may be mediated by the generation of reactive oxygen species (ROS). As these compounds were cytotoxic and induce apoptosis in HL-60 cells, it was considered of to understand the early events that are responsible for this induction of apoptosis like ROS or nitric oxide (NO) generation. Intracellular peroxide in the cells was measured by using flow cytometry by DCFH-DA dye containing 2,7-dichlorodihydrofluorescein diacetate which gets oxidized to the fluorescent compound dichlorofluorescein (DCF) by a variety of peroxides[41] including H_2O_2. Cells were incubated with the test compounds at 1 μM concentration for 24 h in HL-60 cells and analyzed by flow cytometry after double staining with DCFH-DA for fluorescence intensity in FL1 versus cell count (Fig. 7) There was not much any DCF fluorescence (ROS positive cells) in the untreated HL-60 cells, and this status remained unchanged when cells were incubated for 24 h with the compounds **4i**, **4n**, and **5e**. There was a significant increase of ~44% in DCF positive cell population with compound **4h** as compared to the control, whereas compounds **4j** and **4k** induced the

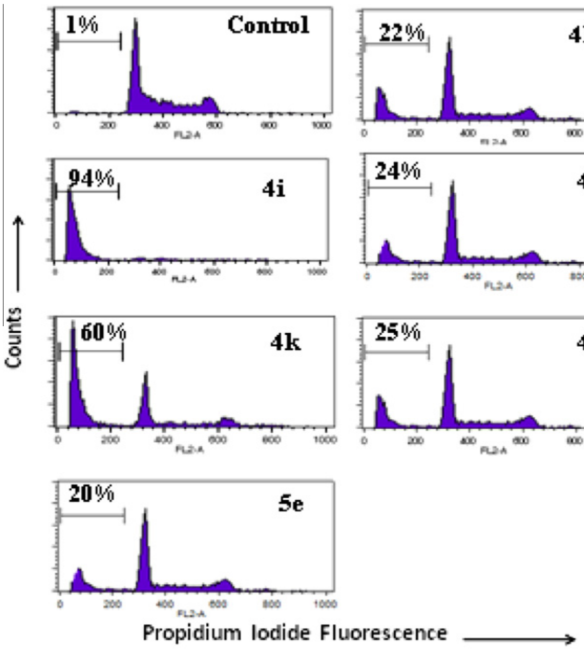

Figure 6a. Flow-activating cell sorting (FACS) analysis of compounds **4h**–**k**, **4n**, and **5e**. Effect of compounds **4h**–**k**, **4n**, and **5e** on cell cycle distribution of HL-60 cell line was examined by staining cells with propidium iodide. Cells were treated with the test compounds at 1 μM and, after 24 h incubation, the percentage of cells in each phase was quantified by using BD-FACS Cell Quest Pro software equipped with electronic doublet discrimination capability laser flow cytometer.

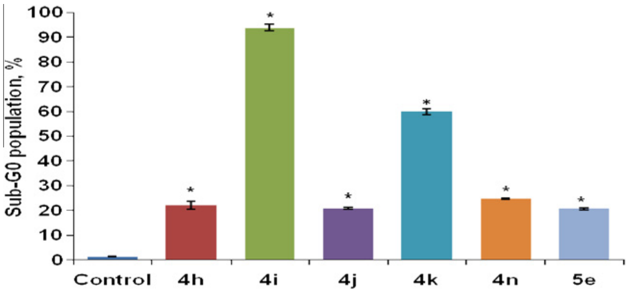

Figure 6b. The histogram depicting the percentage of cells in sub-G0 phases, an indicator of percentage of apoptosis for the compounds **4h**–**k**, **4n**, and **5e**. Data are mean ± SD from three independent experiments. *p*-value: *<0.05 compared to untreated control through ANOVA test.

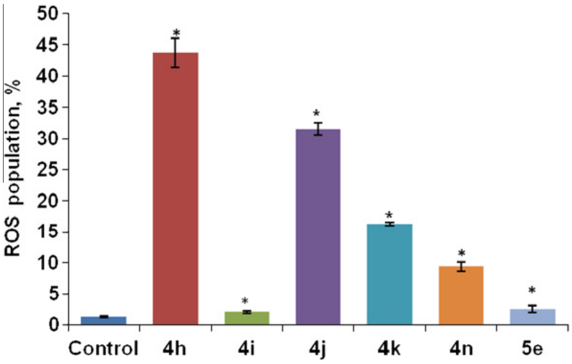

Figure 7. Effect of test compounds on the intracellular levels of ROS on HL-60 cells. The cells (1×10^6 cells, 1.5 mL/plate) were treated with the specified compound 1 μM for 24 h. ROS was measured by the FL-1 channel of FACS Calibur, using the DCF-DA dye. Data are mean ± SD from three independent experiments. *p*-value: *<0.05 compared to untreated control through ANOVA test.

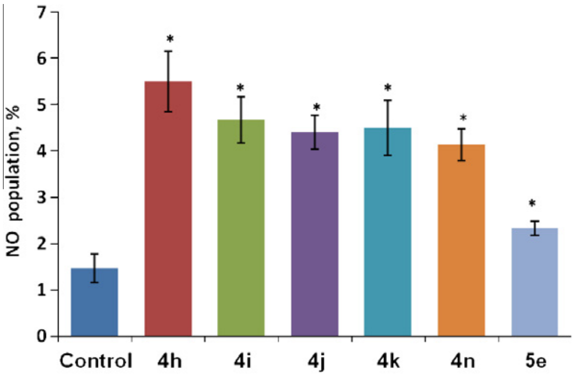

Figure 8. Release of nitric oxide (NO) levels on HL-60 cells was measured as DAF-NO derivative fluorescence intensities. The cells (1×10^6 cells, 1.5 mL/plate) were pre-incubated with DAF-2-DA and then treated with the specified compounds at 1 μM for 24 h. Data are Mean±S.D. from three independent experiments. *p*-value: *<0.05 compared to untreated control through ANOVA test.

generation of peroxide in HL-60 cells (31% and 16% increase, respectively).

2.3.6. Endogenous nitric oxide generation in leukemia cells

To analyze the death pathways induced by these compounds in HL-60 cells, the level of NO induction by employing NO binding dye DAF-2DA was examined. Cells were exposed to the test compounds for 24 h at 1 μM concentration and the NO levels were analyzed by bivariate plots of NO versus counts. None of these compounds induce the level of NO in HL-60 cells; hence the possibility of this event in induction of apoptosis is ruled out (Fig. 8).

2.3.7. Loss of mitochondrial membrane potential

Mitochondria play an essential role in the propagation of apoptosis and its dysfunction within the apoptotic process is often associated with loss of the mitochondrial inner transmembrane potential.[42] Uptake of rhodamine-123 into the mitochondria is driven by mitochondrial trans membrane potential ($\Delta\Psi_{mt}$) that allows the determination of cell population with active integrated mitochondrial functions. Loss of Ψ_{mt} leads to depolarization of mitochondrial membranes leading to collapse of mitochondrial functions ensuing cell death.[43] The loss of Ψ_{mt} indicate loss of mitochondrial integrity to couple electrons to energy production. HL-60 cells exposed to the test compounds for 24 h at 1 μM concentration and were analyzed for Rh-123 uptake by flow cytometry. The percentage of cells with low Rh-123 quantum fluorescence indicates the loss of Ψ_{mt} and was calculated among the total acquired cell events (10,000). In the untreated control cells, more than 90% cells were functionally active with high Rh-123

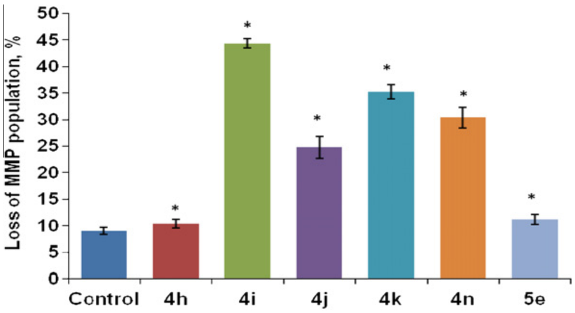

Figure 9. Effect of compounds on mitochondrial membrane potential reduction of HL-60 cells at 1 μM for 24 h was monitored flow cytometrically. Data are mean ± SD from three independent experiments. *p*-value: *<0.05 compared to untreated control through ANOVA test.

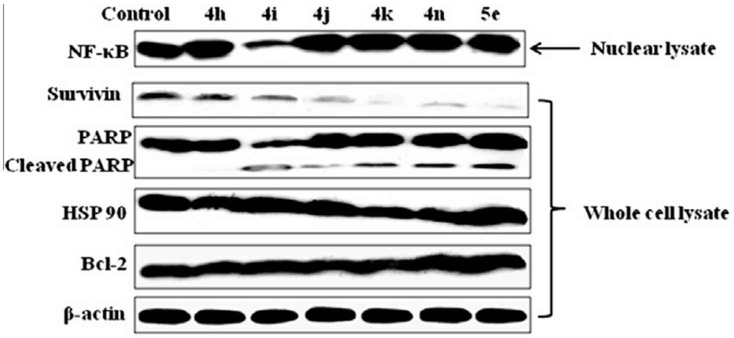

Figure 10. Effect of compounds on the expression level of tumour suppressor and apoptotic specific proteins. HL-60 cells were treated with 1 μM concentration of compounds for 24 h. The cell lysates have been collected and observed the levels of proteins (NF-kB, survivin, PARP, cleaved PARP, HSP 90 and Bcl-2) using specific antibodies. β-Actin was used as a loading control.

signals (Fig. 9). Compound **4i**, **4j**, **4k** and **4n** induce loss of mitochondrial membrane potential in HL-60 cells, amongst them **4i** has the highest potential (45% loss). Thus, decrease in $\Delta\Psi_{mt}$ by the test compounds indicate that the mitochondrial apoptotic death-signal pathway plays a critical role in induction of apoptosis in leukemia cells.

2.3.8. Immunoblot analysis of various cell death targets

NF-κB is a transcriptional factor regulating the expression of several genes in the cells whereas survivin is a cell cycle regulated inhibitor of apoptosis protein (IAP), generally overexpressed in most of the tumours. Suppression of NF-κB activity is required for the induction of apoptotic response, which is a prerequisite in the selection of drugs for the treatment of cancer.[44,45] Both NF-κB and survivin are highly expressed in HL-60 cells. To investigate this effect, cells were treated with test compounds at 1 μM concentration for 24 h and expression of key apoptotic proteins like NF-κB, survivin, poly ADP ribose polymerase (PARP), Bcl-2 and heat shock protein 90 (HSP-90) were analyzed through Western blot. It is observed that compound **4i** significantly inhibits the expression of NF-κB in HL-60 cells, whereas the other compounds have not shown any measurable effect on the NF-κB level (Fig. 10). Some of the tested compounds (**4k**, **4n**, and **5e**) significantly inhibit the survivin level while **4k** has shown maximum inhibition (Fig. 11). During apoptotic stimuli activated caspase-3 appears to cause DNA fragmentation through activation of caspase activated DNase (CAD) in the nucleus of the cells. Activated caspase-3 also utilizes PARP[46] as a substrate and consequently induced its cleavage from 116 to 89 kDa. All the test compounds induce the PARP cleavage whereas **4i** exhibits highest potential in HL-60 cells. Moreover, compound **4k** exhibit significant inhibition of expression of HSP-90 in HL-60 cells. Interestingly cancer cells have a very high level of HSP. These are molecular chaperones expressed constitutively under normal conditions to maintain protein homeostasis and are induced upon environmental stress. Furthermore there are also reports on mitochondrial mediated apoptosis that is involving a down regulation of anti-apoptotic proteins, including Bcl-2 and Bcl-XL.[47] It is interesting to observe that none of the test compounds inhibit the Bcl-2 level in HL-60 cells as evident by the loss of mitochondrial membrane potential by these compounds (Fig. 10).

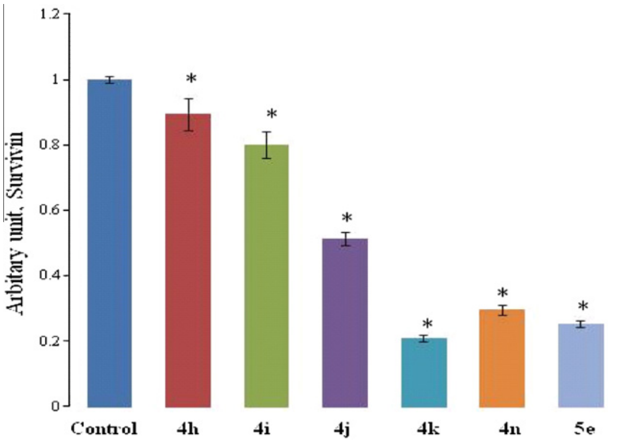

Figure 11. Survivin levels were determined in HL-60 cell lines. The relative density of each survivin band analyzed by Quantity One software of Bio-Rad gel documentation system. A significant decrease in survivin levels was observed by treatment with compounds **4k**, **4n**, and **5e**. Data are Mean±S.D. from three independent experiments. *p*-value: *<0.05 compared to untreated control through ANOVA test.

2.3.9. Scanning electron microscopic (SEM) analysis of cell death induced by compound 4i

SEM examination revealed that HL-60 cells are spherical in shape having microvilli on entire surface and with a few surface projections (Fig. 12B, arrow). Incubation of compound **4i** with these cells at 1 μM concentration after 12 h, caused decrease in the size, smoothening of surface and blebbing of plasma membrane in majority of cells (Fig. 12C–D, asterisk). After 24 h incubation, the apoptotic bodies were seen budding from the cell surface (Fig. 12E, asterisk) and some of the cells were completely transformed into apoptotic bodies (Fig. 12F, arrowhead). However at 0.5 μM concentration apoptosis was seen only in few cells even after 48 h of treatment.

2.3.10. Fluorescence microscopy

Further confirmation of the ability of the most potent compound **4i** to induce apoptosis was obtained by analysis of drug-treated HL-60 and PC-3 cell populations (1 μM, 24 h) by fluorescence microscopy. Following drug treatment morphological changes of HL-60 and PC-3 cells were observed. The untreated cells possess large sized nuclei, whereas the incubation for 24 h at 1 μM concentration of the compound **4i** revealed fragmentation of nuclei due to apoptosis both in PC-3 cells (Fig. 13) and HL-60 (data not shown).

3. Conclusion

In the present study, we synthesized two new series of 2-anilinonicotinyl linked 2-aminobenzothiazole as well as benzothiadiazine conjugates and evaluated them for their antiproliferative activity. It was observed that compound **4i** is 1250 times more active as a cytotoxic agent in cancer cells than in normal cells. Based on their cytotoxic potential, more efficient compounds were

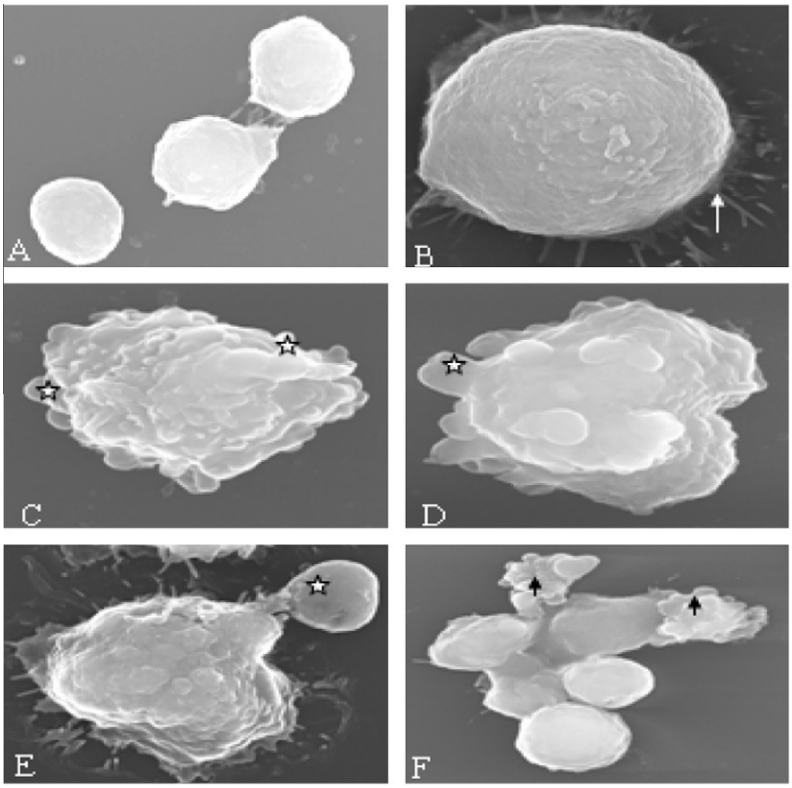

Figure 12. Shows A–F. SEM of control (A, B) and compound **4i** treated (C–F) HL-60 cells showing surface ultra structure. The control cells show microvilli on cell surface (B, arrow), upon treatment (1 μM) after 12 h causes smoothening of cell surface, condensation in size and blebbing of plasma membrane (C–D, asterisk) and after 24 h apoptotic bodies were seen budding from the cell (E, asterisk) and some of the cells were completely transformed into apoptotic bodies (F, arrowhead). (magnification A, F, 4000×, B–E, 8000×).

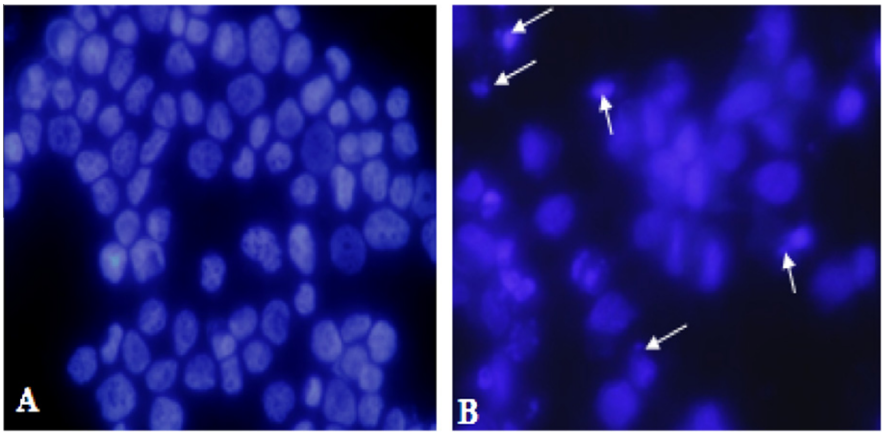

Figure 13. Fluorescent microscopy pictures showing morphological changes in PC-3 cells treated with 1 μM, compound **4i** for 24 h. The cells were stained with DAPI and observed under fluorescent microscope. (A) Untreated control cells showing large sized nuclei. (B) The cells treated for 24 h indicate condensation and fragmentation of nuclei (arrow) due to apoptosis (magnification: A–B, 400×).

further investigated for the possible mechanisms underlying the induction of apoptosis, enhancement of ROS, activation of caspases-3,-8, and -9, and also signals leading to activation of a variety of gene products such as NF-κB, survivin, Hsp-90 inhibition, PARP cleavage proteins which are important in the regulation and execution of apoptosis induced by various stimuli.

Further, studies on induction of apoptosis correlates with the antiproliferative activity in HL-60 cells particularly for compound **4i**. The results of caspase-3 and -9 in a dose-dependent manner suggests that compound **4i** may have induced apoptosis via the traditional nuclear DNA damage pathways.[48,49] It is also evident that compound **4i** induce caspases-3, -8 and -9 activation through both the intrinsic as well as extrinsic apoptotic pathway in HL-60 cells. The loss of mitochondrial membrane potential by some of the compounds and no inhibition on Bcl-2 shows that the Bcl-2 family proteins are not involved in the induction of apoptosis. These compounds did not induce the level of NO in HL-60 cells, which indicates the possibility of other events in apoptosis. SEM studies also confirmed that compound **4i** treated cells led to decrease in size, smoothening of surface and blebbing of plasma membrane in majority of cells which is generally observed in apoptotic cells[50] and also further confirmed by fluorescent microscopic analysis.

4. Experimental section

4.1. Chemistry

All chemicals and reagents were obtained from Aldrich (Sigma–Aldrich, St. Louis, MO, USA), Lancaster (Alfa Aesar, Johnson Matthey Company, Ward Hill, MA, USA) or Spectrochem Pvt. Ltd (Mumbai, India) and were used without further purification. Reactions were monitored by TLC, performed on silica gel glass plates containing 60 GF-254, and visualization on TLC was achieved by UV light or iodine indicator. Column chromatography was performed with Merck 60–120 mesh silica gel. ^{1}H spectra were recorded on Bruker UXNMR/XWIN-NMR (300 MHz) or Inova Varian-VXR-unity (400, 500 MHz) instruments. Chemical shifts (δ) are reported in ppm downfield from internal TMS standard. ESI spectra were recorded on Micro mass, Quattro LC using ESI+ software with capillary voltage 3.98 kV and ESI mode positive ion trap detector. High-resolution mass spectra (HRMS) were recorded on QSTAR XL Hybrid MS/MS mass spectrometer. Melting points were determined with an Electro thermal melting point apparatus, and are uncorrected.

4.2. General procedure

4.2.1. Ethyl 2-(4-methoxyanilino)nicotinate (8a)

2-Chloro nicotinic ethyl ester (**6**, 185 mg, 1 mmol) and 4-methoxy aniline (**7a**, 123 mg, 1 mmol) were heated in ethylene glycol upto 160 °C with stirring for 6 h. Then the reaction mixture was cooled to room temperature and the compound was extracted in ethyl acetate from the aqueous layer and purified by column chromatography (silica gel 60–120) to afford compound **3a** as white solid. Yield 80%; mp 88–90 °C; ^{1}H NMR (200 MHz, $CDCl_3$ + DMSO-d_6): δ 10.00 (s, 1H), 8.32 (dd, J = 4.6, 2.3 Hz, 1H), 8.20 (dd, J = 7.8, 2.3 Hz, 1H), 7.52 (dd, J = 7.0, 2.3 Hz, 2H), 6.88 (dd, J = 7.0, 2.3 Hz, 2H), 6,64 (dd, J = 7.8, 4.6 Hz, 1H), 4.38 (q, J = 7.0 Hz, 2H), 3.82 (s, 3H), 1.43 (t, J = 7.0 Hz, 3H); MS (EI): m/z 272 $[M]^{+}$.

4.2.2. Ethyl 2-(3,4,5-trifluoroanilino)nicotinate (8b)

The compound **8b** was prepared according to the method described for compound **8a**, employing 2-chloro nicotinic ethyl ester (**6**, 185 mg, 1 mmol) and 3,4,5-trifluoroanilino **7b** (147 mg, 1 mmol) to obtain the pure product **3b** as a yellow solid. Yield 77%; mp 92–94 °C; ^{1}H NMR (500 MHz, $CDCl_3$): δ 10.33 (br s, 1H), 8.39 (dd, J = 4.5, 2.2 Hz, 1H), 8.25 (dd, J = 8.3,2.2 Hz, 1H), 7.47 (m, 2H), 6.79 (q, J = 8.3, 5.3 Hz, 1H), 4.38 (q, J = 7.5 Hz, 2H), 1.42 (t, J = 7.5 Hz, 3H); MS (EI): m/z 296 $[M]^{+}$.

4.2.3. Ethyl 2-anilinonicotinate (8c)

The compound **8c** was prepared according to the method described for compound **8a**, employing 2-chloro nicotinic ethyl ester (**6**, 185 mg, 1 mmol) and aniline (**7c**, 93 mg, 1 mmol) to obtain the pure product **8c** as a yellow solid. Yield 72%; mp 54–56 °C; ^{1}H NMR (200 MHz, $CDCl_3$ + DMSO-d_6): δ 10.22 (br s, 1H), 8.34 (dd, J = 4.7, 1.5 Hz, 1H), 8.20 (dd, J = 7.9, 2.3 Hz, 1H), 7.68 (m, 2H), 7.30 (m, 2H), 7.00 (dt, J = 7.1, 1.6 Hz, 1H), 6.66 (dd, J = 7.8, 4.7 Hz, 1H), 4.38 (q, J = 7.0 Hz, 2H), 1.43 (t, J = 7.0 Hz, 3H); MS (EI): m/z 242 $[M]^{+}$.

4.2.4. Ethyl 2-(4-fluoroanilino)nicotinate (8d)

The compound **8d** was prepared according to the method described for compound **8a**, employing 2-chloro nicotinic ethyl ester (**6**, 185 mg, 1 mmol) and 4-fluoroaniline (**7d**, 111 mg, 1 mmol) to obtain the pure product **8d** as a yellow solid. Yield 78%; mp 67–69 °C; ^{1}H NMR (200 MHz, $CDCl_3$ + DMSO-d_6): δ 10.19 (br s, 1H), 8.32 (dd, J = 4.6, 2.0 Hz, 1H), 8.22 (dd, J = 8.0, 2.0 Hz, 1H), 7.65 (m, 2H), 7.00 (m, 2H), 6.70 (dd, J = 7.3, 4.6 Hz, 1H), 4.40 (q, J = 7.3 Hz, 2H), 1.44 (t, J = 7.3 Hz, 3H); MS (EI): m/z 260 $[M]^{+}$.

4.2.5. Ethyl 2-(4-chloroanilino)nicotinate (8e)

The compound **8e** was prepared according to the method described for compound **8a**, employing 2-chloronicotinic ethyl ester (**6**, 185 mg, 1 mmol) and 4-chloroaniline (**7e**, 127 mg, 1 mmol) to obtain the pure product **8e** as a yellow solid. Yield 75%; mp 98–100 °C; ^{1}H NMR (300 MHz, $CDCl_3$ + DMSO-d_6): δ 10.26 (br s, 1H), 8.34 (q, J = 2.6 Hz, 1H), 8.20 (dd, J = 8.3, 2.6, Hz 1H), 7.67 (d, J = 9.0 Hz, 2H), 7.24 (d, J = 9.0 Hz, 2H), 6.70 (dd, J = 7.5, 4.5 Hz, 1H), 4.38 (q, J = 7.5 Hz, 2H), 1.42 (t, J = 7.5 Hz, 3H); MS (EI): m/z 276 $[M]^{+}$.

4.2.6. Ethyl 2-(3-chloro-4-fluoroanilino)nicotinate (8f)

The compound **8f** was prepared according to the method described for compound **8a**, employing 2-chloro nicotinic ethyl ester (**6**, 185 mg, 1 mmol) and 3-chloro- 4-fluoroaniline (**7f**, 145 mg, 1 mmol) to obtain the pure product **8f** as a yellow solid. Yield 83%; mp 54–56 °C; ^{1}H NMR (200 MHz, $CDCl_3$ + DMSO-d_6): δ 10.22 (br s, 1H), 8.34 (dd, J = 4.7, 1.6 Hz, 1H), 8.20 (dd, J = 7.9, 2.3 Hz, 1H), 7.68 (m, 2H), 7.30 (m, 2H), 7.00 (dt, J = 7.1, 1.6 Hz, 1H), 6.66 (dd, J = 7.9, 4.7 Hz, 1H), 4.38 (q, J = 7.1 Hz, 2H), 1.43 (t, J = 7.1 Hz, 3H); MS (EI): m/z 294 $[M]^{+}$.

4.2.7. Ethyl 2-(2,4-dichloroanilino)nicotinate (8g)

The compound **8g** was prepared according to the method described for compound **8a**, employing 2-chloro nicotinic ethyl ester (**6**, 185 mg, 1 mmol) and 2,4-dichloroanilino (**7g**, 162 mg, 1 mmol) to obtain the pure product **3g** as a yellow solid. Yield 81%; mp 96–98 °C; ^{1}H NMR (200 MHz, $CDCl_3$ + DMSO-d_6): δ 10.66 (br s, 1H), 8.38 (q, J = 2.3, 1H), 8.27 (dd, J = 7.8, 2.3 Hz, 1H), 7.40 (d, J = 2.3 Hz, 1H), 7.22 (d, J = 2.3 Hz, 1H), 7.18 (d, J = 2.3 Hz, 1H), 6.78 (dd, J = 7.0, 3.9 Hz, 1H), 4.42 (q, J = 7.0 Hz, 2H), 1.44 (t, J = 7.0 Hz, 3H); MS (EI): m/z 311 $[M]^{+}$.

4.2.8. General procedure for the synthesis of substituted 2-anilino nicotinic acids (9a–g)

2-Anilino nicotino ethylesters (**8a**–**g**, 1 mmol) were refluxed with 2 N NaOH in ethanol for 2 h. The reaction mixture was cooled and left acidified with 2 N HCl to obtain white solid, filtered and washed with water to give pure compounds (**9a**–**g**).

4.2.9. *N3*-[6-(Methyloxy)-1,3-benzothiazol-2-yl]-2-[4-(methyl oxy)phenyl]amino-3-pyridinecarboxamide (4a)

To a stirred solution of 2-(4-methoxyphenylamino) nicotinic acid (**9a**, 244 mg, 1 mmol) in dry DMF (10 mL) hydroxy benzotriazole HOBt (1.2 mmol) were added at 0 °C. After 10 min EDCI (1.2 mmol) was added and finally and 6-methoxy benzo[*d*]thiazol-2-amine (**10a**, 126 mg, 0.7 mmol) were added Then the resulting mixture was stirred at room temperature for 8–10 h and then the reaction mixture was quenched with $NaHCO_3$ and extracted in ethyl acetate (4 × 25 mL) from the ice cold aqueous layer and dried over anhydrous Na_2SO_4. The resulting product was purified by column chromatography employing EtOAc/Hexane as an eluent. Yield 71%; mp 208–210 °C; ^{1}H NMR (200 MHz, $CDCl_3$ + DMSO-d_6): δ 12.49 (br s, 1H), 10.47 (s, 1H), 8.48 (dd, J = 7.6, 1.5 Hz, 1H), 8.27 (dd, J = 4.6, 1.5 Hz, 1H), 7.59 (dd, J = 9.2, 1.5 Hz, 3H), 7.30 (d, J = 2.3 Hz, 1H), 6.95 (dd, J = 8.4, 2.3 Hz, 1H), 6.85 (d, J = 8.4 Hz, 2H), 6.67–6.76 (m, 1H), 3.87 (s, 3H), 3.79 (s, 3H); ^{13}C NMR (75 MHz, CF_3COOD): δ 166.0, 161.3, 154.7, 149.1, 143.7, 131.6, 130.7, 130.3, 126.7, 122.6, 119.5, 119.2, 118.9, 115.6, 115.1, 111.4, 108.9, 68.3, 57.7; MS (ESI): m/z 407 $[M+1]^{+}$; HRMS (ESI m/z) for $C_{21}H_{19}N_4O_3S$, calcd 407.1168, found 407.1177 $[M+1]^{+}$; IR (KBr) (ν_{max}/cm^{-1}): 3276, 2928, 1647, 1605, 1559, 1513, 1470, 1305, 1244, 1140, 1036, 818, 767; Anal. Calcd for $C_{21}H_{18}N_4O_3S$: C, 62.05; H, 4.46; N, 13.78. Found: C, 62.08; H, 4.44; N, 13.76.

4.2.10. *N*3-[6-(Methyloxy)-1,3-benzothiazol-2-yl]-2-[(3,4,5-trifluorophenyl)amino]-3-pyridine carboxamide (4b)

The compound **4b** was prepared according to the method described for compound **4a**, employing 2-(3,4,5-trifluorophenylamino)nicotinic acid (**9b**, 252 mg, 1 mmol) and 6-methoxybenzo[*d*]thiazol-2-amine (**10a**, 126 mg, 0.7 mmol) to obtain the pure product **4b** as a yellow solid. Yield 73%; mp 239–243 °C; ^{1}H NMR (200 MHz, CDCl$_3$ + DMSO-d_6): δ 11.06 (s, 1H), 8.55 (dd, *J* = 7.9, 2.6 Hz, 1H), 8.36 (d, *J* = 2.6 Hz, 1H), 7.74–7.52 (m, 3H), 7.32 (d, *J* = 2.6 Hz, 1H), 6.97 (dd, *J* = 9.2, 2.6 Hz, 1H), 6.94–6.84 (m, 1H), 3.88 (s, 3H); MS (ESI): *m*/*z* 431 [M+1]$^+$; HRMS (ESI *m*/*z*) for $C_{20}H_{14}N_4O_2F_3S$, calcd 431.0802, found 431.0789 [M+1]$^+$; IR (KBr) (ν_{max}/cm^{-1}): 3420, 2924, 1604, 1524, 1468, 1306, 1261, 1040; Anal. Calcd for $C_{20}H_{13}F_3N_4O_2S$: C, 55.81; H, 3.04; N, 13.02. Found: C, 55.84; H, 3.02; N, 13.01.

4.2.11. *N*3-[6-(Methyloxy)-1,3-benzothiazol-2-yl]-2(phenylamino)-3-pyridine carboxamide (4c)

The compound **4c** was prepared according to the method described for compound **4a**, employing 2-(phenylamino) nicotinic acid (**9c**, 214 mg, 1 mmol) and 6-methoxybenzo[*d*]thiazol-2-amine (**10a**, 126 mg, 0.7 mmol) to obtain the pure product **4c** as a yellow solid. Yield 68%; mp 158–160 °C; ^{1}H NMR (200 MHz, CDCl$_3$ + DMSO-d_6): δ 10.67 (s, 1H), 8.47 (dd, *J* = 7.8, 2.2 Hz, 1H), 8.32 (dd, *J* = 5.1, 2.2 Hz, 1H), 7.75 (d, *J* = 1.5 Hz, 2H), 7.57(d, *J* = 8.7 Hz, 1H), 7.28 (t, *J* = 7.8 Hz, 3H), 6.98 (t, *J* = 3.6 Hz, 1H), 6.94 (d, *J* = 2.9 Hz, 1H), 6.70–6.82 (m, 1H), 3.88 (s, 3H); ^{13}C NMR (75 MHz, DMSO-d_6): δ 170.4, 168.3, 155.4, 154.7, 151.7, 143.0, 139.8, 138.9, 131.7, 128.6, 122.0, 120.0, 119.4, 115.4, 113.6, 110.7, 105.6, 63.57; MS (ESI): *m*/*z* 377 [M+1]$^+$; HRMS (ESI *m*/*z*) for $C_{20}H_{17}N_4O_2S$, calcd 377.1086, found 377.1072 [M+1]$^+$; IR (KBr) (ν_{max}/cm^{-1}): 3317, 3002, 2969, 2927, 2829, 1686, 1621, 1580, 1507, 1250; Anal. Calcd for $C_{20}H_{16}N_4O_2S$: C, 63.81; H, 4.28; N, 14.88. Found: C, 63.79; H, 4.30; N, 14.84.

4.2.12. *N*3-[6-(Methyloxy)-1,3-benzothiazol-2-yl]-2-[(4-fluorophenyl)amino]-3-pyridine carboxamide (4d)

The compound **6d** was prepared according to the method described for compound **6a**, employing 2-(4-fluorophenylamino)nicotinic acid (**9d**, 232 mg, 1 mmol) and 6-methoxybenzo[*d*]thiazol-2-amine (**10a**, 126 mg, 0.7 mmol) to obtain the pure product **4d** as a yellow solid. Yield 78%; mp 203–206 °C; ^{1}H NMR (200 MHz, CDCl$_3$ + DMSO-d_6): δ 12.61 (s, 1H), 10.69 (s, 1H), 8.49 (dd, *J* = 8.3, 1.5 Hz, 1H), 8.30 (dd, *J* = 5.3, 2.3 Hz, 1H), 7.78–7.65 (m, 2H), 7.56 (d, *J* = 8.3 Hz, 1H), 7.33 (d, *J* = 2.3 Hz, 1H), 7.00 (t, *J* = 8.3 Hz, 3H), 6.84–6.73 (m, 1H), 3.87 (s, 3H); MS (ESI): *m*/*z* 395 [M+1]$^+$; HRMS (ESI *m*/*z*) for $C_{20}H_{16}N_4O_2FS$, calcd 395.0960, found 395.0978 [M+1]$^+$; IR (KBr) (ν_{max}/cm^{-1}): 3437, 3292, 2925, 1650, 1608, 1556, 1512, 1464, 1268, 812; Anal. Calcd for $C_{20}H_{15}FN_4O_2S$: C, 60.90; H, 3.83; N, 14.20. Found: C, 60.85; H, 3.85; N, 14.18.

4.2.13. *N*3-[6-(Methyloxy)-1,3-benzothiazol-2-yl]-2-[(4-chlorophenyl)amino]-3-pyridine carboxamide (4e)

The compound **4e** was prepared according to the method described for compound **4a**, employing 2-(4-chlorophenylamino)nicotinic acid (**9e**, 249 mg, 1 mmol) and 6-methoxybenzo[*d*]thiazol-2-amine (**10a**, 126 mg, 0.7 mmol) to obtain the pure product **4e** as a yellow solid. Yield 75%; mp 222–224 °C; ^{1}H NMR (200 MHz, CDCl$_3$+DMSO-d_6): δ 12.43 (br s, 1H), 10.63 (s, 1H), 8.41 (dd, *J* = 8.1, 2.2 Hz, 1H), 8.26 (dd, *J* = 5.1, 2.2 Hz, 1H), 7.63 (d, *J* = 8.8 Hz, 2H), 7.53 (d, *J* = 8.8 Hz, 1H), 7.23 (t, *J* = 2.9 Hz, 2H), 7.17 (d, *J* = 2.2 Hz, 1H), 6.93 (dd, *J* = 8.8, 2.9 Hz, 1H), 6.69–6.80 (m, 1H), 3.81 (s, 3H); ^{13}C NMR (75 MHz, CDCl$_3$+DMSO-d_6): δ 159.1, 151.7, 151.2, 148.2, 138.7, 136.2, 134.8, 133.9, 127.1, 122.7, 122.3, 120.4, 118.2, 114.7, 114.7, 112.4, 106.4, 56.18; MS (ESI): *m*/*z* 411 [M+1]$^+$; HRMS (ESI *m*/*z*) for $C_{20}H_{16}ClN_4O_2S$, calcd 411.0669, found 411.0682 [M+1]$^+$; IR (KBr) (ν_{max}/cm^{-1}): 3377, 2925, 1735, 1647, 1605, 1551, 1513, 1476, 1407, 1305, 1265, 1233, 1140, 1088, 815, 769; Anal. Calcd for $C_{20}H_{15}ClN_4O_2S$: C, 58.46; H, 3.68; N, 13.64. Found: C, 58.53; H, 3.63; N, 13.65.

4.2.14. *N*3-[6-(Methyloxy)-1,3-benzothiazol-2-yl]-2-[(4-chloro-3-fluorophenyl)amino]-3-pyridine carboxamide (4f)

The compound **4f** was prepared according to the method described for compound **4a**, employing 2-(3-chloro-4-fluorophenylamino)nicotinic acid (**9f**, 267 mg, 1 mmol) and 6-methoxybenzo[*d*]thiazol-2-amine (**10a**, 126 mg, 0.7 mmol) to obtain the pure product **4f** as a yellow solid. Yield 74%; mp 230–234 °C; ^{1}H NMR (200 MHz, CDCl$_3$+DMSO-d_6): δ 10.83 (br s, 1H), 8.60(d, *J* = 7.8 Hz, 1H), 8.35 (d, *J* = 5.2 Hz, 1H), 8.07 (dd, *J* = 6.5, 2.6 Hz, 1H), 7.68–7.49 (m, 2H), 7.33 (d, *J* = 2.6 Hz, 1H), 7.13 (t, *J* = 9.1 Hz, 1H), 7.03 (dd, *J* = 9.1, 2.6 Hz, 1H), 6.92–6.79 (m, 1H), 3.89 (s, 3H); MS (ESI): *m*/*z* 429 [M+1]$^+$; HRMS (ESI *m*/*z*) for $C_{20}H_{15}N_4O_2FSCl$ calcd 429.0606, found 429.0598 [M+1]$^+$; IR (KBr) (ν_{max}/cm^{-1}): 3421, 2925, 1659, 1604, 1517, 1464, 1302, 1261, 761; Anal. Calcd for $C_{20}H_{14}ClFN_4O_2S$: C, 56.01; H, 3.29; N, 13.06. Found: C, 56.08; H, 3.27; N, 13.05.

4.2.15. *N*3-[6-(Methyloxy)-1,3-benzothiazol-2-yl]-2-[(2,4-dichlorophenyl)amino]-3-pyridine carboxamide (4g)

The compound **4g** was prepared according to the method described for compound **4a**, employing 2-(2,4-dichlorophenylamino)nicotinic acid (**9g**, 283 mg, 1 mmol) and 6-methoxy benzo[*d*]thiazol-2-amine (**10a**, 126 mg, 0.7 mmol) to obtain the pure product **4g** as a yellow solid. Yield 72%; mp 208–210 °C; ^{1}H NMR (200 MHz, DMSO-d_6): δ 12.58 (s, 1H), 11.07 (s, 1H), 8.67 (d, *J* = 8.8 Hz, 1H), 8.57 (dd, *J* = 8.1, 2.2 Hz, 1H), 8.35 (dd, *J* = 4.4, 1.5 Hz, 1H), 7.60 (t, *J* = 8.8 Hz, 1H), 7.39 (d, *J* = 2.2 Hz, 1H), 7.30 (d, *J* = 2.2 Hz, 1H), 7.18 (dd, *J* = 8.8, 2.2 Hz, 1H), 6.95 (dd, *J* = 8.8, 2.9 Hz, 1H), 6.87 (dd, *J* = 8.1, 4.4 Hz, 1H); MS (ESI): *m*/*z* 445 [M+1]$^+$; HRMS (ESI *m*/*z*) for $C_{20}H_{15}Cl_2N_4O_2S$, calcd 445.0285, found 445.0293 [M+1]$^+$; IR (KBr) (ν_{max}/cm^{-1}): 3421, 2925, 1660, 1604, 1516, 1464, 1301, 1260, 761; Anal. Calcd for $C_{20}H_{14}Cl_2N_4O_2S$: C, 53.94; H, 3.17; N, 12.58. Found: C, 53.88; H, 3.19; N, 12.5.

4.2.16. *N*3-(6-Nitro-1,3-benzothiazol-2-yl)-2-(4-methoxyanilino)nicotinamide (4h)

The compound **4h** was prepared according to the method described for compound **4a**, employing 2-(4-methoxyphenylamino)nicotinic acid (**9a**, 244 mg, 1 mmol) and 6-nitrobenzo[*d*]thiazol-2-amine (**10b**, 137 mg, 0.7 mmol) to obtain the pure product **4h** as a yellow solid. Yield 71%; mp 249–251 °C; ^{1}H NMR (200 MHz, CDCl$_3$+DMSO-d_6): δ 13.0 (br s, 1H), 10.36 (s, 1H), 8.81 (s,1H), 8.52 (d, *J* = 7.1 Hz, 1H), 8.36–8.24 (m, 2H), 7.81 (d, *J* = 9.5 Hz, 1H), 7.56 (d, *J* = 8.7 Hz, 2H), 6.85 (d, *J* = 9.5 Hz, 2H), 6.78–6.69 (m, 1H), 3.77 (s, 3H); ^{13}C NMR (75 MHz, CF$_3$COOD): δ 169.2, 166.6, 162.8, 154.7, 149.4, 148.41, 143.9, 143.5, 130.6, 130.3, 127.2, 126.5, 122.4, 121.9, 119.9, 119.1, 118.6, 115.6, 114.9, 111.1; MS (ESI): *m*/*z* 422 [M+1]$^+$; HRMS (ESI *m*/*z*) for $C_{20}H_{16}N_5O_4S$, calcd 422.0926, found 422.0923 [M+1]$^+$; IR (KBr) (ν_{max}/cm^{-1}): 3380, 2931, 1653, 1620, 1575, 1511, 1451, 1339, 1250; Anal. Calcd for $C_{20}H_{15}N_5O_4S$: C, 57.00; H, 3.59; N, 16.62. Found: C, 57.08; H, 3.56; N, 16.59.

4.2.17. *N*3-(6-Nitro-1,3-benzothiazol-2-yl)-2-[(3,4,5-trifluorophenyl)amino]-3-pyridine carboxamide (4i)

The compound **6i** was prepared according to the method described for compound **4a**, employing 2-(3,4,5-trifluorophenyl amino)nicotinic acid (**9b**, 252 mg, 1 mmol) and 6-nitrobenzo[*d*]thiazol-2-amine (**10b**, 137 mg,0.7 mmol) to obtain the pure product **4i** as a yellow solid. Yield 70%; mp 235–237 °C; ^{1}H NMR (500 MHz, CDCl$_3$+Acetone-d_6): δ 10.71 (br s, 1H), 8.86 (d,

J = 2.9 Hz, 1H), 8.64 (d, J = 6.8 Hz, 1H), 8.49 (dd, J = 4.9, 1.9 Hz, 1H), 8.32 (dd, J = 8.8, 1.9 Hz, 1H), 7.86 (d, J = 8.8 Hz, 1H), 7.68–7.61 (m, 2H), 6.99 (dd, J = 7.8, 4.9 Hz, 1H); ^{13}C NMR (75 MHz, CF_3COOD): δ 169.2, 166.7, 154.3, 149.9, 148.5, 144.1, 143.9, 130.5, 127.3, 122.5, 122.1, 120.3, 118.8, 116.9, 115.6, 115.0, 111.1; MS (ESI): m/z 446 [M+1]$^+$; HRMS (ESI m/z) for $C_{19}H_{11}F_3N_5O_3S$, calcd 446.0529, found 446.0535 [M+1]$^+$; IR (KBr) (ν_{max}/cm^{-1}): 3322, 3100, 2928, 1659, 1524, 1441, 1341, 1284, 1135, 1044; Anal. Calcd for $C_{19}H_{10}F_3N_5O_3S$: C, 51.24; H, 2.26; N, 15.72. Found: C, 51.17; H, 2.24; N, 15.71.

4.2.18. *N*3-(6-Nitro-1,3-benzothiazol-2-yl)-2-(phenylamino)-3-pyridine carboxamide (4j)

The compound **4j** was prepared according to the method described for compound **4a**, employing 2-(phenylamino)nicotinic acid (**9c**, 214 mg, 1 mmol) and 6-nitrobenzo[*d*]thiazol-2-amine (**10b**, 137 mg, 0.7 mmol) to obtain the pure product **4j** as a yellow solid. Yield 75%; mp 233–237 °C; ^{1}H NMR (200 MHz, $CDCl_3$+ DMSO-d_6): δ 10.52 (s, 1H), 8.77 (d, J = 2.1, 1H), 8.50 (dd, J = 7.9, 1.4 Hz, 1H), 8.37 (dd, J = 5.0, 2.2 Hz, 1H), 8.27 (dd, J = 9.3, 2.2 Hz, 2H), 7.85–7.67 (m, 2H), 7.32 (t, J = 8.6 Hz, 2 H), 7.03 (t, J = 7.2 Hz, 1H), 6.86–6.74 (m, 1H); ^{13}C NMR (75 MHz, CF_3COOD): δ 166.2, 162.7, 154.1, 149.5, 1439, 133.8, 122.4, 121.4, 121.1, 120.2, 118.7, 115.5, 114.9, 114.4, 111.8, 111.2; MS (ESI): m/z 392 [M+1]$^+$; HRMS (ESI m/z) for $C_{19}H_{14}N_5O_3S$ calcd 392.0808, found 392.0817 [M+1]$^+$; IR (KBr) (ν_{max}/cm^{-1}): 3376, 2925, 1653, 1519, 1444, 1305, 1259, 1121; Anal. Calcd for $C_{19}H_{13}N_5O_3S$: C, 58.30; H, 3.35; N, 17.89. Found: C, 58.24; H, 3.36; N, 17.83.

4.2.19. *N*3-(6-Nitro-1,3-benzothiazol-2-yl)-2-(4-fluoroanilino)nicotinamide(4k)

The compound **4k** was prepared according to the method described for compound **4a**, employing 2-(4-fluoro phenylamino)nicotinic acid **9d**, 232 mg, 1 mmol) and 6-nitrobenzo[*d*] thiazol-2-amine (**10b**, 137 mg, 0.7 mmol) to obtain the pure product **4k** as a yellow solid. Yield 72%; mp 239–241 °C; ^{1}H NMR (200 MHz, $CDCl_3$+DMSO-d_6): δ 10.23 (s, 1H), 9.08 (d, J = 2.9 Hz, 1H), 8.47 (dd, J = 8.0, 1.5 Hz, 1H), 8.38 (dd, J = 5.1, 2.2 Hz, 1H), 8.32 (dd, J = 9.4, 2.9 Hz, 1H), 7.90 (d, J = 5.1 Hz, 1H), 7.72 (dd, J = 9.4, 5.1 Hz, 2H), 7.17 (t, J = 9.4 Hz, 2H), 6.98–6.89 (m, 1H); ^{13}C NMR (75 MHz, DMSO-d_6): δ 168.5, 166.4, 154.7, 152.0, 142.7, 139.1, 136.2, 131.8, 122.1, 122.0, 121.8, 119.3, 118.8, 115.5, 114.9, 113.6, 110.3; MS (ESI): m/z 410 [M+1]$^+$ HRMS (ESI m/z) for $C_{19}H_{13}N_5O_3FS$, calcd 410.0737, found 410.0723 [M+1]$^+$; IR (KBr) (ν_{max}/cm^{-1}): 3377, 3060, 1654, 1621, 1587, 1508, 1450, 1340, 1217; Anal. Calcd for $C_{19}H_{12}FN_5O_3S$: C, 55.74; H, 2.95; N, 17.11. Found: C, 55.79; H, 2.98; N, 17.10.

4.2.20. *N*3-(6-Nitro-1,3-benzothiazol-2-yl)-2-(4-chloroanilino)nicotinamide(4l)

The compound **4l** was prepared according to the method described for compound **4a**, employing 2-(4-chlorophenyl amino)nicotinic acid (**9e**, 249 mg, 1 mmol) and 6-nitrobenzo[*d*]thiazol-2-amine (**10b**, 137 mg, 0.7 mmol) to obtain the pure product **4l** as a yellow solid. Yield 70%; mp 288–290 °C Charred; ^{1}H NMR (300 MHz, $CDCl_3$+DMSO-d_6): δ 11.1 (s, 1H), 8.97 (br s, 1H), 8.46 (d, J = 7.7 Hz, 1H), 8.36 (d, J = 2.6, 1H), 8.26 (d, J = 8.5 Hz, 1H), 7.81 (t, J = 8.9 Hz, 3H), 7.38 (d, J = 8.5 Hz, 2H), 6.99–6.89 (m, 1H); ^{13}C NMR (75 MHz, DMSO-d_6): δ 168.3, 166.2, 154.5, 142.6, 140.3, 139.0, 136.1, 131.7, 122.3, 122.3, 112.1, 121.8, 120.0, 118.7, 115.4, 114.8, 113.4, 111.2; MS (ESI): m/z 426 [M+1]$^+$; HRMS (ESI m/z) for $C_{19}H_{13}ClN_5O_3S$, calcd 426.0419, found 426.0428 [M+1]$^+$; IR (KBr) (ν_{max}/cm^{-1}): 3374, 3061, 2925, 1657, 1621, 1520, 1342, 760; Anal. Calcd for $C_{19}H_{12}ClN_5O_3S$: C, 53.59; H, 2.84; N, 16.45. Found: C, 53.57; H, 2.86; N, 16.44%

4.2.21. *N*3-(6-Nitro-1,3-benzothiazol-2-yl)-2-(3-chloro-4-fluoroanilino)nicotinamide (4m)

The compound **4m** was prepared according to the method described for compound **4a**, employing 2-(3-chloro-4-fluorophenylamino)nicotinic acid (**9f**, 267 mg, 1 mmol) and 6-nitrobenzo[*d*]thiazol-2-amine (**10b**, 137 mg, 0.7 mmol) to obtain the pure product **4m** as a yellow solid. Yield 74%; mp 258–260 °C; ^{1}H NMR (500 MHz, $CDCl_3$+ Acetone-d_6): δ 10.71 (br s, 1H), 8.86 (d, J = 2.9 Hz, 1H), 8.64 (dd, J = 8.8, 1.9 Hz, 2H), 8.49 (dd, J = 4.9, 2.9 Hz, 1H), 8.35–8.31 (m, 1H), 7.86 (d, J = 8.8 Hz, 1H), 7.71 (s, 1H), 7.68–7.62 (m,2H), 6.99 (dd, J = 7.8, 4.9 Hz, 1H); MS (ESI): m/z 444 [M+1]$^+$; HRMS (ESI m/z) for $C_{19}H_{12}ClFN_5O_3S$, calcd 444.0326, found 444.0333 [M+1]$^+$; IR (KBr) (ν_{max}/cm^{-1}): 3277, 3103, 2927, 1648, 1610, 1575, 1531, 1341, 1313, 1285, 1126, 760; Anal. Calcd for $C_{19}H_{11}ClFN_5O_3S$: C, 51.42; H, 2.50; N, 15.78. Found: C, 51.49; H, 2.8; N, 15.77.

4.2.22. *N*3-[6-(Nitro-1,3-benzothiazol-2-yl]-2-[(2,4-dichlorophenyl)amino]-3-pyridine carboxamide (4n)

The compound **6n** was prepared according to the method described for compound **4a**, employing 2-(2,4-dichlorophenylamino)nicotinic acid (**9g**, 283 mg, 1 mmol) and 6-nitrobenzo[*d*]thiazol-2-amine (**10b**, 137 mg, 0.7 mmol) to obtain the pure product **4n** as a yellow solid. Yield 71%; mp 268–270 °C; ^{1}H NMR (200 MHz, $CDCl_3$+DMSO-d_6): δ 10.93 (s, 1H), 8.85 (d, J = 2.2 Hz, 1H), 8.66 (d, J = 8.8 Hz, 2H), 8.60 (dd, J = 8.0, 1.5 Hz, 1H), 8.39 (dd, J = 5.1, 1.5 Hz, 1H), 8.26 (dd, J = 9.5, 2.2 Hz, 1H), 7.84 (t, J = 8.8 Hz, 1H), 7.42 (d, J = 2.2 Hz, 1H), 7.22 (dd, J = 8.8, 2.2 Hz, 1H), 6.99–6.89 (m, 1H); ^{13}C NMR (75 MHz, $CDCl_3$+ Acetone-d_6): δ 166.7, 158.3, 153.8, 151.1, 142.5, 137.4, 135.1, 127.9, 127.5, 126.1, 125.3, 122.9, 121.5, 120.0, 119.9, 113.65, 113.5, 113.2, 109.7, 107.0, 106.7; MS (ESI): m/z 460 [M+1]$^+$ HRMS (ESI m/z) for $C_{19}H_{12}Cl_2N_5O_3S$, calcd 460.0028, found 460.0038 [M+1]$^+$; IR (KBr) (ν_{max}/cm^{-1}): 3333, 1660, 1615, 1523, 1340, 1283, 757; Anal. Calcd for $C_{19}H_{11}Cl_2N_5O_3S$: C, 49.58; H, 2.41; N, 15.21. Found: C, 49.66; H, 2.39; N, 15.19.

4.2.23. 2-[2-(4-Methoxyanilino)-3-pyridyl]-10-methyl-5,10-dihydro-5λ6-benzo[*e*][1,2,4]triazolo[1,5-*b*][1,2,4]thiadiazine-5,5-dione (5a)

3-Hydrazino-4-methyl-4*H*-1,2,4-benzothiadiazine1,1-dioxide (11a, 158 mg, 0.7 mmol) and 2-(4-methoxyphenylamino) nicotinic acid (9a, 244 mg, 1 mmol) was taken in phosphorus oxychloride (5 mL) and refluxed for 4–5 h in an oil bath under nitrogen atmosphere. The reaction mixture was then cooled to room temperature, poured onto crushed ice and neutralized with sodium bicarbonate. The aqueous layer was extracted with ethyl acetate (4 × 50 mL), dried over anhydrous Na_2SO_4 and concentrated under vacuum to get the title compound. The resulting product was purified by recrystalization from methanol. Yield 65%; mp 232–234 °C; ^{1}H NMR (300 MHz, DMSO-d_6+Acetone-d_6): δ 9.87 (br s, 1H), 8.53 (dd, J = 9.4, 1.9 Hz, 1H), 8.33 (dd, J = 4.5, 1.9 Hz, 1H), 8.28 (dd, J = 8.5, 1.3 Hz, 1H), 8.03 (dt, J = 8.6, 1.3 Hz, 1H), 7.83 (d, J = 8.5 Hz, 1H), 7.71 (d, J = 8.9 Hz, 2H), 7.61 (t, J = 7.7 Hz, 1H), 7.01–6.91 (m, 1H), 4.04 (s,3H), 3.80 (s, 3H); MS (ESI): m/z 435 [M+1]$^+$; HRMS (ESI m/z) for $C_{21}H_{19}N_6O_3S$, calcd 435.1230, found 435.1239 [M+1]$^+$; IR (KBr) (ν_{max}/cm^{-1}): 3322, 3225, 3141, 2924, 1590, 1510, 1443, 1350, 1238, 1179, 761; Anal. Calcd for $C_{21}H_{18}N_6O_3S$: C, 58.05; H, 4.18; N, 19.34. Found: C, 58.09; H, 4.15; N, 19.38.

4.2.24. 10-Methyl-2-[2-(3,4,5-trifluoroanilino)-3-pyridyl]-5,10-dihydro-5λ6-benzo[*e*] [1,2,4]triazolo [1,5-*b*][1,2,4]thiadiazine-5,5-dione (5b)

The compound 5b was prepared according to the method described for compound 5a, employing 2-(3,4,5-trifluoro phenylamino)nicotinic acid (9b, 252 mg, 1 mmol) and 3-hydrazino-4-methy-

4*H*-1,2,4-benzothiadiazine 1,1-dioxide (11a, 158 mg, 0.7 mmol) to obtain the pure product 5b as a white solid. Yield 65%; mp 250–254 °C; ^{1}H NMR (200 MHz, $CDCl_3$+DMSO-d_6): δ 9.99 (s, 1H), 8.46(d, *J* = 7.8 Hz, 1H), 8.28(d, *J* = 3.9 Hz, 1H), 8.08 (d, *J* = 7.8 Hz, 1H), 7.91–7.72 (m, 1H); 7.66–7.31 (m, 4H), 6.94–6.79 (m, 1H), 3.89 (s,3H); MS (ESI): *m*/*z* 459 $[M+1]^+$; HRMS (ESI *m*/*z*) for $C_{20}H_{14}N_6O_2$,F_3S calcd 459.0836, found 459.0851 $[M+1]^+$; IR (KBr) (ν_{max}/cm^{-1}): 3425, 3316, 3148, 1646, 1587, 1563, 1523, 1441, 1355, 1186, 756; Anal. Calcd for $C_{20}H_{13}F_3N_6O_2S$: C, 52.40; H, 2.86; N, 18.33. Found: C, 52.35; H, 2.83; N, 18.30.

4.2.25. 2-(2-Anilino-3-pyridyl)-10-methyl-5,10-dihydro-5λ6-benzo[*e*][1,2,4]triazolo[1,5-*b*][1,2,4]thiadiazine-5,5-dione (5c)

The compound 5c was prepared according to the method described for compound 5a, employing 2-(phenyl amino)nicotinic acid (9c, 214 mg, 1 mmol) and 3-hydrazino-4-methy-4*H*-1,2,4-benzothiadiazine 1,1-dioxide (11a, 158 mg, 0.7 mmol) to obtain the pure product 5c as a white solid. Yield 62%; mp 246–248 °C; ^{1}H NMR (200 MHz, $CDCl_3$ +DMS0-d_6): $\delta\delta$ 9.91(br s, 1H), 8.51 (dd, *J* = 7.5, 1.7 Hz, 1H), 8.32 (dd, *J* = 5.0, 1.7 Hz, 1H), 8.17 (dd, *J* = 8.3, 1.7 Hz, 1H), 7.86 (dt, *J* = 8.3, 6.6 Hz, 1H), 7.75 (d, *J* = 7.5 Hz, 3H), 7.52–7.44 (m, 2H), 7.35 (t, *J* = 8.3 Hz, 1H), 7.03 (t, *J* = 7.5 Hz, 1H), 6.90–6.81 (m, 1H), 3.97 (s, 3H); ^{13}C NMR (75 MHz, DMSO-d_6) δ 156.2, 154.7, 151.7, 139.9, 138.9, 131.8, 131.7, 128.6, 122.0, 120.0, 119.5, 119.4, 119.3, 115.1, 113.6, 110.7, 105.0, 55.6; MS (ESI): *m*/*z* 405 $[M+1]^+$; HRMS (ESI *m*/*z*) for $C_{20}H_{17}N_6O_2S$, calcd 405.1123, found 405.1133 $[M+1]^+$; IR (KBr) (ν_{max}/cm^{-1}): 3310, 3218, 3143, 3025, 1630, 1585, 1562, 1497, 1445, 1392, 1346, 1178, 1127, 760; Anal. Calcd for $C_{20}H_{16}N_6O_2S$: C, 59.39; H, 3.99; N, 20.78. Found: C, 59.45; H, 3.96; N, 20.75.

4.2.26. 2-[2-(4-Chloroanilino)-3-pyridyl]-10-methyl-5,10-dihydro-5λ6-benzo[*e*][1,2,4]triazolo[1,5-*b*][1,2,4]thiadiazine-5,5-dione (5d)

The compound 5d was prepared according to the method described for compound 11a, employing 2-(4-chloro phenylamino) nicotinic acid (9e, 249 mg, 1 mmol and 3-hydrazino-4-methy-4*H*-1,2,4-benzothiadiazine 1,1-dioxide (10a, 158 mg, 0.7 mmol) to obtain the pure product 5d as a white solid. Yield 64%; mp 218–220 °C; ^{1}H NMR (200 MHz, $CDCl_3$) δ 9.93 (br s, 1H), 8.52 (dd, *J* = 7.7, 2.6 Hz, 1H), 8.32 (dd, *J* = 5.1, 2.6 Hz, 1H), 8.14 (d, *J* = 7.7 Hz, 1H), 7.86 (t, *J* = 9.0 Hz, 1H), 7.74 (d, *J* = 9.0 Hz, 2H), 7.52–7.38 (m, 2H), 7.28 (d, *J* = 9.0 Hz, 2H), 6.86 (dd, *J* = 7.7, 5.1 Hz, 1H), 3.97 (s, 3H); MS (ESI): *m*/*z* 439 $[M+1]^+$; HRMS (ESI *m*/*z*) for $C_{20}H_{16}ClN_6O_2S$, calcd 439.0742, found 439.0743 $[M+1]^+$; IR (KBr) (ν_{max}/cm^{-1}): 3311, 3215, 3133, 1589, 1490, 1441, 1354, 1308, 1178, 823, 759, 603; Anal. Calcd for $C_{20}H_{15}ClN_6O_2S$: C, 54.73; H, 3.44; N, 19.15. Found: C, 54.68; H, 3.42; N, 19.16.

4.2.27. 2-[2-(2,4-Dichloroanilino)-3-pyridyl]-10-methyl-5,10-dihydro-5λ6-benzo[*e*][1,2,4]triazolo [1,5-*b*][1,2,4]thiadiazine-5,5-dione (5e)

The compound 5e was prepared according to the method described for compound 5a, employing 2-(2,4-dichloro phenylamino)nicotinic acid (7 g, 283 mg, 1 mmol) and 3-hydrazino-4-methy-4*H*-1,2,4-benzothiadiazine1,1-dioxide (10a, 158 mg, 0.7 mmol) to obtain the pure product 5e as a white solid. Yield 76%; mp 260–262 °C Charred; ^{1}H NMR (200 MHz, $CDCl_3$+DMSO-d_6): δ 10.49 (br s, 1H), 8.95 (d, *J* = 8.7 Hz, 1H), 8.62 (dd, *J* = 7.7, 1.9 Hz, 1H), 8.46 (dd, *J* = 4.8, 1.9 Hz, 1H), 8.27 (d, *J* = 8.7 Hz, 1H), 8.02 (t, *J* = 8.7 Hz, 1H), 7.82 (d, *J* = 7.7 Hz, 1H), 7.64–7.58 (m, 2H), 7.42 (dd, *J* = 8.7, 1.9 Hz, 1H), 7.14 (dd, *J* = 7.7, 4.9 Hz, 1H), 4.02 (s, 3H); ^{13}C NMR (75 MHz, CF_3COOD): δ 160.4, 156.5, 151.9, 151.7, 147.9, 140.2, 139.1, 138.7, 138.6, 135.6, 133.8, 131.8, 131.7, 130.4, 127.1, 126.7, 122.5, 118.7, 116.8, 116.3, 115., 111.3, 111.0, 36.04; MS (ESI): *m*/*z* 473 $[M+1]^+$; HRMS (ESI *m*/*z*) for $C_{20}H_{15}Cl_2N_6O_2S$, calcd 473.0349, found 473.0354 $[M+1]^+$; IR (KBr) (ν_{max}/cm^{-1}): 3290, 3198, 3106, 1594, 1562, 1439, 1339, 1311, 1174, 763; Anal. Calcd for $C_{20}H_{14}Cl_2N_6O_2S$: C, 50.75; H, 2.98; N, 17.75. Found: C, 50.71; H, 2.99; N, 17.71.

4.2.28. 2-[2-(4-Methoxyphenyl)-3-pyridyl]-10-phenyl-5,10-dihydro-5λ6-benzo[*e*][1,2,4]triazolo [1,5-*b*][1,2,4]thiadiazine-5,5-dione (5f)

The compound **5f** was prepared according to the method described for compound 5a, employing 2-(4-methoxy phenylamino)nicotinic acid (9a, 244 mg, 1 mmol) and 3-hydrazino-4-phenyl-4*H*-1,2,4-benzothiadiazine 1,1-dioxide (11b, 201 mg, 0.7 mmol)to obtain the pure product 11f as a white solid. Yield 65%; mp 223–234 °C; ^{1}H NMR (300 MHz, $CDCl_3$): δ 9.70 (br s, 1H), 8.34 (dd, *J* = 7.7, 1.9 Hz, 1H), 8.24 (dd, *J* = 4.7, 1.9 Hz, 1H), 8.18 (dd, *J* = 8.1, 1.5 Hz, 1H), 7.76–7.68 (m, 3H), 7.63–7.49 (m, 1H), 7.41 (t, *J* = 8.9 Hz, 3H), 6.84 (d, *J* = 8.9 Hz, 3H), 6.72–6.65 (m, 1H), 3.81 (s, 3H); MS (ESI): *m*/*z* 497 $[M+1]^+$; HRMS (ESI *m*/*z*) for $C_{26}H_{21}N_6O_3S$, calcd 497.1382, found 497.1396 $[M+1]^+$; IR (KBr) (ν_{max}/cm^{-1}): 3325, 3143, 2920, 1594, 1508, 1444, 1355, 1232, 1165, 765; Anal. Calcd for $C_{26}H_{20}N_6O_3S$: C, 62.89; H, 4.06; N, 16.93. Found: C, 62.84; H, 4.04; N, 16.92.

4.2.29. 10-Phenyl-2-[2-(3,4,5-trifluoroanilino)-3-pyridyl]-5,10-dihydro-5λ6-benzo[*e*] [1,2,4]triazolo[1,5-*b*][1,2,4]thiadiazine-5,5-dione (5g)

The compound 5 g was prepared according to the method described for compound 5a, employing 2-(3,4,5-trifluoro phenylamino)nicotinic acid (9b, 252 mg, 1 mmol) and 3-hydrazino-4-phenyl-4*H*-1,2,4-benzothiadiazine 1,1-dioxide (11b, 201 mg, 0.7 mmol) to obtain the pure product 5 g as a white solid. Yield 70%; mp 290–293 °C charred; ^{1}H NMR (200 MHz, $CDCl_3$+DMSO-d_6): δ 10.21(s, 1H), 8.47–8.37 (m, 1H), 8.32–8.22 (m, 1H), 8.20–8.08 (m, 1H), 7.83–7.40 (m, 8H); 7.12–6.98 (m, 1H), 6.89–6.76 (m, 1H); MS (ESI): *m*/*z* 521 $[M+1]^+$; HRMS (ESI *m*/*z*) for $C_{25}H_{16}F_3N_6O_2S$, calcd 521.1001, found 521.1008 $[M+1]^+$; IR (KBr) (ν_{max}/cm^{-1}): 3423, 3315, 3143, 1644, 1587, 1564, 1525, 1440, 1355, 1186, 757 cm^{-1}; Anal. Calcd for$C_{25}H_{15}F_3N_6O_2S$: C, 57.69; H, 2.90; N, 16.15. Found: C, 57.62; H, 2.93; N, 16.17.

4.2.30. 2-(2-Anilino-3-pyridyl)-10-phenyl-5,10-dihydro-5λ6-benzo[*e*] [1,2,4]triazolo[1,5-*b*][1,2,4]thiadiazine-5,5-dione (5h)

The compound **5h** was prepared according to the method described for compound **5a**, employing 2-(phenyl amino)nicotinic acid (**9c**, 214 mg, 1 mmol) and 3-hydrazino-4-phenyl-4*H*-1,2,4-benzothiadiazine 1,1-dioxide (**11b**, 201 mg, 0.7 mmol) to obtain the pure product **11h** as a white solid. Yield 66%; mp 233–234 °C charred; ^{1}H NMR (300 MHz, $CDCl_3$): δ 9.96 (br s, 1H), 8.40 (dd, *J* = 8.3, 2.3 Hz, 1H), 8.29 (dd, *J* = 5.3, 2.3 Hz, 1H), 8.19 (dd, *J* = 7.5, 1.5 Hz, 1H), 7.78–7.70 (m, 3H), 7.66–7.39 (m, 6H), 7.31–7.25 (m, 3H), 6.98 (t, *J* = 8.3 Hz, 1H), 6.87 (d, *J* = 8.3 Hz, 1H), 6.79–6.71 (m, 1H); ^{13}C NMR (75 MHz, $CDCl_3$): δ 161.1, 153.3, 152.5, 150.1, 140.5, 137.6, 137.3, 136.3, 134.7, 130.9, 130.3, 129.0, 128.6, 124.6, 124.1, 121.8, 119.7, 117.3, 113.6, 107.9; MS (ESI): *m*/*z* 467 $[M+1]^+$; HRMS (ESI *m*/*z*) for $C_{25}H_{19}N_6O_2S$, calcd 467.1271, found 467.1290 $[M+1]^+$; IR (KBr) (ν_{max}/cm^{-1}): 3326, 3216, 3138, 3049, 2923, 1562, 1493, 1438, 1349, 1183, 751, 696, 659;. Anal. Calcd for $C_{25}H_{18}N_6O_2S$: C, 64.36; H, 3.89; N, 18.01. Found: C, 64.43; H, 3.86; N, 18.02.

4.2.31. 2-[2-(4-Chloroanilino)-3-pyridyl]-10-phenyl-5,10-dihydro-5λ6-benzo[*e*][1,2,4]triazolo[1,5-*b*][1,2,4]thiadiazine-5,5-dione (5i)

The compound **5i** was prepared according to the method described for compound **11a**, employing 2-(4-chlorophenylamino) nicotinic acid (**9e**, 249 mg, 1 mmol and 3-hydrazino-4-phenyl-4*H*-1,2,4-benzothiadiazine 1,1-dioxide (**11b**, 201 mg, 0.7 mmol) to obtain the pure product **5i** as a white solid. Yield 65%; mp 241–243 °C; ^{1}H NMR (200 MHz, CDCl$_3$): δ 9.95 (br s, 1H), 8.16 (d, J = 4.4, Hz, 1H), 8.01–7.93 (m, 2H), 7.88–7.68 (m, 3H), 7.69–7.51 (m, 4H), 7.49–7.33 (m, 1H), 7.29–7.20 (m, 2H), 6.82–6.54 (m, 2H), 6.49–6.36 (m, 1H); MS (ESI): m/z 501 [M+1]$^+$; HRMS (ESI m/z) for $C_{25}H_{18}ClN_6O_2S$, calcd 501.0890, found 501.0901 [M+1]$^+$; IR (KBr) (ν_{max}/cm^{-1}): 3318, 3146, 1646, 1585, 1563, 1522, 1441, 1353, 1316, 1185, 755; Anal. Calcd for $C_{25}H_{17}ClN_6O_2S$: C, 59.94; H, 3.42; N, 16.78. Found: C, 59.99; H, 3.40; N, 16.75.

4.2.32. 2-[2-(2,4-Dichloroanilino)-3-pyridyl]-10-phenyl-5,10-dihydro-5λ6-benzo[*e*][1,2,4]triazolo[1,5-*b*][1,2,4]thiadiazine-5,5-dione (5j)

The compound **5j** was prepared according to the method described for compound **5a**, employing 2-(2,4-dichlorophenyl amino) nicotinic acid (**4g**, 283 mg, 1 mmol) and 3-hydrazino-4-phenyl-4*H*-1,2,4-benzothiadiazine 1,1-dioxide (**11b**, 201 mg, 0.7 mmol) to obtain the pure product **5j** as a white solid. Yield 68%; mp 272–275 °C Charred; ^{1}H NMR (300 MHz, CDCl$_3$) δ 10.01 (br s, 1H), 8.43 (dd, J = 8.3, 2.3 Hz, 1H), 8.29 (dd, J = 4.5, 1.5 Hz, 1H), 8.18 (d, J = 7.5 Hz, 1H), 7.77–7.37 (m, 5H), 7.02 (t, J = 9.1 Hz, 1H),6.87 (d, J = 8.3 Hz, 1H), 6.83–6.76 (m, 1H); ^{13}C NMR (75 MHz, CF$_3$COOD): δ = 159.6, 156.1, 151.8, 147.6, 140.1, 139.6, 139.4, 138.3, 137.5, 135.4, 133.8, 133.5, 131.8, 131.1, 130.8, 130.4, 127.7, 126.5, 126.4, 122.8, 120.8, 118.6, 116.7, 115.6, 114.9, 111.1; MS (ESI): m/z 534 [M]$^+$; HRMS (ESI m/z) for $C_{25}H_{17}Cl_2N_6O_2S$, calcd 535.0525, found 535.0510 [M+1]$^+$; IR (KBr) (ν_{max}/cm^{-1}): 3280, 3197, 3102, 1610, 1557, 1517, 1476, 1438, 1355, 1355, 1313, 1187, 766; Anal. Calcd for $C_{25}H_{16}Cl_2N_6O_2S$: C, 56.08; H, 3.01; N, 15.70. Found: C, 56.14; H, 3.03; N, 15.67.

4.3. Biology

4.3.1. Cell culture

The human cell lines used in the studies were grown in their respective medium supplemented with 10% heat-inactivated fetal bovine serum (FBS), penicillin (100 units/ml), streptomycin (100 µg/mL), L-glutamine (0.3 mg/mL), pyruvic acid (0.11 mg/mL), 0.37% NaHCO$_3$ and 50 µM of 2-mercaptoethanol at 37 °C in an atmosphere of 95% air and 5% CO$_2$ with 98% humidity. Cells grown in monolayer cultures were trypsinized with trypsin (0.1% w/v)/EDTA (1 mM) solution. Cells grown in semi-confluent stage (approx. 70% confluent) or in logarithmic phase were treated with tested molecules dissolved in DMSO while the untreated control cultures received only the vehicle (DMSO, <0.5% v/v).

4.3.2. Drugs and chemicals

The human cell lines used in the studies were procured from either National Centre for Cell Sciences (NCCS), Pune, India or National Cancer Institute, Frederick, U.S.A.

4.3.3. Cell proliferation assay using MTT

The cells were plated in 96-well plates at a density of 2.0×10^4 in 200 µl of medium per well of 96 well plate. Cultures were incubated with different concentrations of test material and incubated for 48 h. The medium was replaced with fresh medium containing 100 µg/ml of 3-(4,5-dimethylthiazol-2-yl)-2,5-diphenyltetrazolium bromide (MTT) for 2–3 h. The supernatant was aspirated and MTT-formazan crystals dissolved in 100 µl DMSO; OD measured at λ 540 nm (reference wavelength, λ 620 nm) on ELISA reader Cell viability % was calculated by comparing the absorbance of treated versus untreated cells.

4.3.4. DNA agarose gel electrophoresis

Apoptosis was also assessed by electrophoresis of extracted genomic DNA from cells. Briefly, 2×10^6 cells after various treatments were centrifuged at 100×*g* for 10 min, and washed in PBS containing 20 mM EDTA. The pellet was lysed in 250 µl of lysis buffer (100 mM NaCl, 5 mM EDTA, 10 mM Tris–HCl, pH 8.0, 5% Triton X-100) containing 400 µg/ml DNase-free RNase and incubated at 37 °C for 90 min followed by 1 h incubation with proteinase-K (200 µg/mL) at 50 °C for 1 h. The DNA was extracted with 150 µl of phenol for 1 min and centrifuged 13000xg for 2 min. The aqueous phase was further extracted with phenol:chloroform:isoamyl alcohol (25:24:1) and centrifuged. DNA was precipitated from aqueous phase with 3 volumes of chilled alcohol and 0.3 M sodium acetate at 20 °C overnight. The precipitate was centrifuged at 13000×*g* for 10 min. The DNA pellet was washed in 80% alcohol, dried, dissolved in 50 µl TE buffer, mixed in loading buffer and electrophoresed in 1.8% agarose gel at 50 V for 1.5 h in TAE buffer.

4.3.5. Flow cytometric analysis of apoptosis and necrosis using Annexin V/PI dual staining

All measurements were performed on a FACS-Calibur (Becton Dickinson USA), equipped with a 488 nm argon-ion laser, using Cell Quest software. Detection of apoptosis by Annexin V-FITC was performed using Annexin V-FITC Apoptosis Detection Kit from Santa Cruz Biotech, according to the manufacturer's instruction. Cells (1×10^6/1.5 mL medium/12 well plate) were treated with different doses of test molecules for indicated time periods, were washed twice with PBS and then resuspended in100 µl of the binding buffer provided with the apoptosis detection kit. Cells were stained with annexinV-FITC antibody and PI and scanned for fluorescence intensity in (FL-1; λ_{em}: 530 nm) for FITC and (FL-2; λ_{em}: 585 nm) for PI channels. The fraction of cell population in different quadrants was analyzed using quadrant statistics. Cells in the lower right quadrant represented apoptosis and in the upper right quadrant represented post apoptotic necrosis. To set up the flow cytometer apoptosis-induced cells stained with FITC only and labeled with PI only, respectively, were used.

4.3.6. DNA content and cell cycle phase distribution

Cells (1×10^6/1.5 ml medium/12 well plate) were treated with indicated doses of test material were collected, washed in PBS, fixed in 70% cold ethanol and placed at −20 °C overnight. Cells were washed with PBS, subjected to RNase digestion (400 µg/ml) at 37 °C for 45 min. Finally, cells were incubated with propidium iodide (10 µg/ml) for 30 min and analyzed immediately on flow cytometer FACS Calibur (Becton Dickinson, USA). The subG0/G1 peak represents the apoptotic cells population. Data were collected in list mode on 10,000 events for FL2-A versus FL2-W. Apoptotic nuclei appear as a broad hypodiploid DNA peak at lower fluorescence intensity compared to nuclei in G0/G1 phase.

4.3.7. Measurement of Caspase-9, Caspase-8 and Caspase-3 activity

Cells (2×10^6) were incubated with test material for the indicated concentrations and time periods. At the end of treatment cells were washed in PBS and pellet lysed in cell lysis buffer. Activities of caspase-3, -8 and -9 in the cell lysates were determined fluorometrically using BD Apoalert caspase fluorescent assay kits. Caspase-3 and -8 employed fluorochome conjugated peptides DEVD-AFC and IETD-AFC as substrates, respectively while caspase-9 employed LEHD-AMC. Release of AFC (7-amino-4-trifluoromethyl coumarin) and AMC (7-aminomethylcoumarin) were assayed according to the instructions provided in the Manual by the supplier. Specific inhibitors were used as negative control to determine whether fluorescence intensity changes were specific for the activity of caspases. The peptide based inhibitors used were DEVD-CHO for caspase-3, IETD-fmk for caspase-8 and LEHD-CHO for caspase-9.

4.3.8. Flow cytometeric analysis of reactive oxygen species (ROS)

Cells (1×10^6/1.5 mL medium/12 well plate) were treated with indicated doses of cells treated with test material and untreated controls were incubated for 30 min in a CO_2 incubator with 10 μM of 2'7'-dichlorodihydrofluorescein diacetate (H_2DCFDA). The dye was removed by centrifugation and washing with PBS (2×). The pellets were resuspended in adequate volume of PBS (0.5 ml/sample) and transferred to polypropylene tubes and placed into a water-bath (37 °C). To estimate intracellular peroxide production, fluorescence intensity (FL-1; λ_{em}: 530 nm) was recorded. Cells incubated with carboxy-H_2DCFDA only were employed to monitor basal peroxide synthesis. Fluorescence intensity was expressed in Dot plot quadrants. The percentage of cells producing ROS (% DCF +ve) was determined with Cell Quest Pro software (BD Biosciences) and presented in histogram analysis.

4.3.9. Flow cytometric analysis of intracellular nitric oxide using DAF-2-DA

Cells (1×10^6/1.5 mL medium/12 well plate) were incubated for 30 min with diaminofluorescein 2-diacetate (DAF-2-DA)(10 μM) before the treatment of test material. Cells were collected, washed in PBS and analyzed on flow cytometer in FL-1 channel for evaluation of NO positive cell population.

4.3.10. Measurement of mitochondrial membrane potential

Cells (1×10^6/ 1.5 mL medium/12 well plate) after various treatments were incubated with medium containing rhodamine-123 (5 μg/mL; stock, 1 mg/mL PBS) for 1 h. Cells were washed in PBS and centrifuged at 100×*g* for 5 min and suspended in sheath fluid. Immediately before analysis, propidium iodide (5 μg/mL; stock 1 mg/ml PBS) was added to the samples. The intensity of fluorescence from 10,000 events was analyzed in FL-1 channel on flow cytometer.

4.3.11. Immunoblotting

4.3.11.1. Preparation of total cell lysate. Cells (2×10^6) after treatment with test material were harvested and resuspended in 0.2 ml of RIPA buffer (50 mM Tris–HCl, pH 7.4, 150 mM NaCl, 1% Triton X-100, 0.1% SDS, 5 mM EDTA, 30 mM Na_2HPO_4, 50 mM NaF, 0.5 mM $NaVO_4$, 2 mM phenylmethylsulfonyl fluoride, and 10% protease cocktail inhibitor). Cells were incubated on ice for 30 min, vortexed and centrifuged at 12000×*g* for 15 min. Supernatants were collected and stored at −80 °C. The protein contents were determined using Bradford reagent (Bio-Rad protein assay kit) and aliquots normalized to equal quantities before loading.

4.3.11.2. Preparation of nuclear extracts. Cells (5×10^6) after treatment with test material were harvested and resuspended in 400 μL ice-cold hypotonic buffer (10 mM HEPES/KOH pH 7.9, 2 mM $MgCl_2$, 0.1 mM EDTA, 10 mM KCl, 1 mM DTT, 0.5 mM PMSF, 1% (v/v) eukaryotic protease inhibitor cocktail) for 10 min on ice. Suspension was vortexed and centrifuged at 15000×*g* for 30 s and supernatant discarded, the nuclear pellet was resuspended in to 100 μl of ice cold saline buffer (50 mM HEPES/KOH pH7.9, 50 mM KCl, 300 mM NaCl, 0.1 mM EDTA, 10% glycerol, 1 mM DTT, 0.5 mM PMSF, 1% (v/v) eukaryotic protease inhibitor cocktail) on ice for 20 min. The suspension was vortexed and centrifuged at 15000×*g* for 5 min at 4 °C and the supernatant used as nuclear fraction are incubated with test molecules for the desired time periods. At the end of treatment cells are collected and washed twice with PBS (100×*g*, 5 min, 4 °C) and suspend in 400 μL ice cold hypotonic buffer for 10 min on ice. Suspension is vortexed and centrifuged at 15000×*g* for 30 s at 4 °C .The supernatant is discarded and the nuclear pellet gently resuspended in to 100 μL of ice cold saline buffer on ice for 20 min. Cells suspension is vortexed and centrifuged at 15000×*g* for 5 min at 4 °C. The supernatant is stored at −70 °C as nuclear lysate and their protein contents assayed.

4.3.11.3. Protein estimation. Bio-Rad protein assay kit solvent (5×) is diluted to 1× with HPLC grade water and filtered through whatman filter no 1. Add 190 μL of this reagent into each well of 96 well plates and to this add 50 μL of protein sample, mix and wait for 5 min. Read the absorbance at 595 nm on Elisa plate reader. A standard plot of BSA (1–100 μg) is drawn using same procedure and slope of the straight line determined. Amount of sample protein is calculated through the standard calibration plot of BSA.

4.3.11.4. Western Blot analysis. The protein lysates along with standard protein marker are subjected to discontinuous SDS–PAGE analysis. Proteins aliquots (50 μg) are resolved on SDS–PAGE, run at 60 V (PowerPac^{TM} HC High current power supply, BioRad), for 3 h. The resolved proteins were electro transferred to polyvinylidene difluoride (PVDF) membranes (Bio-RAD) into Western blotting transfer frames in the following manner: Sponge-Blotting paper-gel-PVDF membrane–western blotting paper-sponge and transfer overnight at 4 °C at 30 V in transfer buffer. Non-specific bindings of the membrane are blocked by incubation with 5% non-fat milk in Tris-buffered saline (10 mM Tris–HCl, 150 mM NaCl) containing 0.1% Tween-20 (TBST) for 1 h at room temperature. The blots are probed with respective primary anti-human antibodies for 2 h (1:1000 dilutions) and washed three times with TBST. The blots are then incubated with horseradish peroxidase conjugated respective secondary antibodies for 1 h (1:1000 dilution), washed again three times with TBST. PVDF membrane was incubated in to ECL Pus western blot detection reagent (ECL kit, Amersham Biosciences) for 5 min on a transparency sheet, in dark. PVDF membrane was placed into the Hyper Cassette and superimposed with high performance chemiluminescence's film in the dark room, wait for the 2 min and develop the protein signal on to the high performance chemiluminescence's X-ray film by using developer and fix the signal by processing chemical fixer. Wash out the film with tap water gently and dry. The density of the bands was arbitrarily quantified using Quantity One Software of Bio-RAD gel documentation system.

4.3.12. Morphological analysis by Scanning Electron Microscopy (SEM)

The HL-60 cells were seeded in 6-well tissue culture plates at the density of 2×10^5 cells per ml in complete medium supplemented with 10% FCS in the presence and absence (as controls) of compound **4i** at 0.5 and 1 μM for 24–48 h. After 24 h, culture was incubated with the compound **4i** for 6, 12, 24 and 48 h. The stock solution was prepared in DMSO and added to the medium to achieve the desired final concentration. Control samples were treated with DMSO vehicle alone. To assess the mechanism of cell death, after incubation for specified time at 37 °C, the cells were processed for SEM studies. For SEM, HL-60 cells were sedimented at 1800 rpm for 10 min. Cell pellets were fixed immediately with 2.5% glutaraldehyde in 0.1 M phosphate buffer (pH 7.2) at 4 °C for 1 h, post-fixed with 1% OsO_4 for 1 h in the same buffer, dehydrated with graded ethanol solutions and dried in a critical point drier using CO_2 (Blazer's Union) and coated with gold using a Sputter coater (Polaron). The specimens were examined with a JEOL-100CXII electron microscope with ASID at 40 KV

4.3.13. DAPI staining of cells for nuclear morphology

The mechanism of cell death was also studied in HL-60 and PC-3 cells by fluorescent microscopic studies. The PC-3 cells were treated with compd. as in case of HL-60 cells. For fluorescent DAPI staining, air dried smears of cells on glass slides were fixed in absolute methanol at −20 °C for 20 min and stained with DAPI (Sigma) at 1 μg/mL at room temperature for 20 min in the dark and mounted with 90% glycerol in PBS and observed under fluorescent microscope (Olympus).

Acknowledgments

The authors Y.V.V.S and M.A. are thankful to UGC, and M.K.R, F.S thankful to CSIR, New Delhi, India for the award of research fellowships.

References and notes

1. Gastman, B. R. *Head Neck* **2001**, 409.
2. Zhang, H. Z.; Kasibhatla, S.; Kuemmerle, J.; Kemnitzer, W.; Ollis-Mason, K.; Qiu, L.; Crogan-Grundy, C.; Tseng, B.; Drewe, J.; Cai, S. X. *J. Med. Chem.* **2005**, *48*, 5215.
3. Mattson, M. P. *Brain Pathol.* **2000**, *2*, 300.
4. Kumar, S. *Cell Death Differ.* **2007**, *14*, 32.
5. Thornberry, N. A. *Chem. Biol.* **1998**, *5*, R97.
6. Koyanagi, N.; Nagasu, T.; Fujita, F.; Watanabe, T.; Tsukahara, K.; Funahashi, Y.; Fujita, M.; Taguchi, T.; Yoshino, H.; Kitoh, K. *Cancer Res.* **1994**, *54*, 1702.
7. Yokoi, A.; Kuromitsu, J.; Kawai, T.; Nagasu, T.; Sugi, N. H.; Yoshimatsu, K.; Yoshino, H.; Owa, T. *Mol. Cancer Ther.* **2002**, *1*, 275.
8. Yoshimatsu, K.; Yamaguchi, A.; Yoshino, H.; Koyanagi, N.; Kitoh, K. *Cancer Res.* **1997**, *57*, 3208.
9. Mauer, A. M.; Cohen, E. E.; Ma, P. C.; Kozloff, M. F.; Schwartzberg, L.; Coates, A. I.; Qian, J.; Hagey, A. E.; Gordon, G. B. *J. Thorac. Oncol.* **2008**, *3*, 631.
10. Cai, S. X.; Nguyen, B.; Jia, S.; Herich, J.; Guastella, J.; Reddy, S.; Tseng, B.; Drewe, J.; Kasibhatla, S. *J. Med. Chem.* **2003**, *46*, 2474.
11. Kamal, A.; Khan, M. N. A.; Reddy, K. S.; Rohini, K. *Bioorg. Med. Chem.* **2007**, *15*, 1004.
12. Abdel-Rahman, H. M.; Morsy, M. A. *J. Enzyme Inhib. Med. Chem.* **2007**, *22*, 57.
13. Hutchinson, A.; Chua, M.; Browne, H. L.; Trapani, V.; Bradshaw, T. D.; Westwell, A. D.; Stevens, M. F. *J. Med. Chem.* **2001**, *44*, 1446.
14. Kashiyama, E.; Hutchinson, I.; Chua, M. S.; Stinson, S. F.; Phillips, L. R.; Kaur, G.; Sausville, E. A.; Bradshaw, T. D.; Westwell, A. D.; Stevens, M. F. *J. Med. Chem.* **1999**, *42*, 4172.
15. Mortimer, C. G.; Wells, G.; Crochard, J. P.; Stone, E. L.; Bradshaw, T. D.; Stevens, M. F.; Westwell, A. D. *J. Med. Chem.* **2006**, *49*, 179.
16. Chua, M. S.; Shi, D. F.; Wrigley, S.; Bradshaw, T. D.; Hutchinson, I.; Shaw, P. N.; Barrett, D. A.; Stanley, L. A.; Stevens, M. F. *J. Med. Chem.* **1999**, *42*, 381.
17. Trapani, V.; Patel, V.; Leong, C. O.; Ciolino, H. P.; Yeh, G. C.; Hose, C.; Trepel, J. B.; Stevens, M. F.; Sausville, E. A.; Loaiza-Pérez, A. I. *Br. J. Cancer* **2003**, *8*, 599.
18. Shi, D. F.; Bradshaw, T. D.; Wrigley, S.; McCall, C. J.; Lelieveld, P.; Fichtner, I.; Stevens, M. F. *J. Med. Chem.* **1996**, *39*, 3375.
19. Bradshaw, T. D.; Westwell, A. D. *Curr. Med. Chem.* **2004**, *11*, 1009.
20. Vullo, D.; Franchi, M.; Gallori, E.; Antel, J.; Scozzafava, A.; Supuran, C. T. *J. Med. Chem.* **2004**, *47*, 1272.
21. Tzanopoulou, S.; Sagnou, M.; Paravatou-Petsotas, M.; Gourni, E.; Loudos, G.; Xanthopoulos, S.; Lafkas, D.; Kiaris, H.; Varvarigou, A.; Pirmettis, I. C.; Papadopoulos, M.; Pelecanou, M. *J. Med. Chem.* **2010**, *53*, 4633.
22. Caleta, I.; Kralj, M.; Marjanović, M.; Bertosa, B.; Tomić, S.; Pavlović, G.; Pavelić, K.; Karminski-Zamola, G. *J. Med. Chem.* **2009**, *52*, 1744.
23. Larner, J. In *Goodman and Gilman's The Pharmacological Basic of Therapeutics*; Gilman, A. G., Goodman, L. S., Gilman, A., Eds., sixth ed.; Macmillan Publishing Co. Inc.: New York, 1980; p 1510.
24. Howbert, J. J.; Grossmann, C. S.; Crowell, T. A.; Rieder, B. J.; Harper, R. W.; Kramer, K. E.; Tao, E. V.; Aikins, J.; Poore, G. A.; Rinzel, S. M.; Grindey, G. B.; Shaw, W. W.; Todd, G. C. *J. Med. Chem.* **1990**, *33*, 2393.
25. Houghton, P. J.; Bailey, F. C.; Germain, G. S.; Grindey, G. B.; Howbert, J. J.; Houghton, J. A. *Biochem. Pharmacol.* **1990**, *39*, 1187.
26. Houghton, P. J.; Bailey, F. C.; Germain, G. S.; Grindey, G. B.; Witt, B. C.; Houghton, J. A. *Cancer Res.* **1990**, *50*, 318.
27. Houghton, P. J.; Bailey, F. C.; Houghton, J. A.; Murti, K. G.; Howbert, J. J.; Grindey, G. B. *Cancer Res.* **1990**, *50*, 664.
28. Rush, G. F.; Rinzel, S.; Boder, G.; Heim, R. A.; Toth, J. E.; Ponsler, G. D. *Biochem. Pharmacol.* **1992**, *44*, 2387.
29. Kamal, A.; Khan, M. N. A.; Reddy, K. S.; Srikanth, Y. V. V.; Sridhar, B. *Chem. Biol. Drug. Des.* **2008**, *71*, 78.
30. Kamal, A.; Khan, M. N. A.; Srikanth, Y. V. V.; Rajesh, S. V. C. R. N. C. *Chem. Biol. Drug. Des.* **2009**, *73*, 687.
31. Kamal, A.; Khan, M. N. A.; Srikanth, Y. V. V.; Reddy, K. S.; Juvekar, A.; Sen, S.; Kurian, N.; Zingde, S. *Bioorg. Med. Chem.* **2008**, *16*, 7804.
32. Kamal, A.; Tekumalla, V.; Krishnan, A.; Bhadra, M. P.; Bhadra, U. *Chem. Med. Chem.* **2008**, *3*, 794.
33. Kamal, A.; Reddy, J. S.; Ramaiah, M. J.; Dastagiri, D.; Bharathi, E. V.; Sagar, M. V. P.; Pushpavalli, S. N.; Ray, P.; Bhadra, M. P. *Med. Chem. Commun.* **2010**, *1*, 355.
34. Kamal, A.; Dastagiri, D.; Ramaiah, M. J.; Reddy, J. S.; Bharathi, E. V.; Srinivas, C.; Pal, D.; Bhadra, M. P. *Chem. Med. Chem.* **2010**, *5*, 1937.
35. Kamal, A.; Srikanth, Y. V. V.; Khan, M. N. A.; Shaik, T. B.; Ashraf, M. *Bioorg. Med. Chem. Lett.* **2010**, *20*, 5229.
36. Reddy, A. V. N.; Kamal, A.; Sattur, P. B. *Indian J. Chem* **1985**, *24B*, 1295.
37. Vichai, V.; Kirtikara, K. *Nat. Protoc.* **2006**, *1*, 1112.
38. (a) Slater, T. *Biochem. Biophys. Acta.* **1963**, *77*, 383; (b) van de Loosdrecht, A. A. J. *Immunol. Methods* **1994**, *174*, 311; (c) Alley, M. C. *Cancer Res.* **1988**, *48*, 589.
39. Ziegler, A.; Groscurth, P. *News Physiol. Sci.* **2004**, *19*, 124.
40. Saraste, A.; Pulkki, K. *Cardivascular Res.* **2000**, *45*, 528.
41. (a) Cai, J.; Jones, D. P. *J. Biol. Chem.* **1998**, *273*, 11401; (b) Nohl, H.; Gille, L.; Staniek, K. *Biochem. Pharmacol.* **2005**, *69*, 719.
42. Ly, J. D.; Grubb, D. R.; Lawen, A. *Apoptosis* **2003**, *3*, 115.
43. Green, D. R.; Kroemer, G. *Science* **2005**, *305*, 626.
44. Shishodia, S.; Amin, H.; Lai, R.; Aggarwal, B. B. *Biochem. Pharmacol.* **2005**, *70*, 700.
45. Viatour, P.; Merville, M. P.; Bours, V.; Chariot, A. *Trends. Biochem. Sci.* **2005**, *30*, 43.
46. Soldani, C.; Scovassi, A. I. *Apoptosis* **2002**, *7*, 321.
47. Sasayama, T.; Kazuhiro, K.; Mizukawa, A.; Kawamura, T.; Kondoh, K.; Hosoda, E.; Kohmura, J. *Neurooncology* **2007**, *85*, 123.
48. Chen, C. Y.; Chen, C. H.; Lo, Y. C.; Wu, B. N.; Wang, H. M.; Lo, W. L.; Yen, C. M.; Lin, R. J. *J. Nat. Prod.* **2008**, *71*, 933.
49. Bose, J. S.; Gangan, V.; Prakash, R.; Jain, S. K.; Manna, S. K. *J. Med. Chem.* **2009**, *52*, 3184.
50. Lion, C. J.; Matthews, C. S.; Stevens, M. F.; Westwell, A. D. *J. Med. Chem.* **2005**, *48*, 1292.